

1. Report No. FHWA/TX-91+1205-4F		2. Government Accession No.		3. Recipient's Catalog No.	
4. Title and Subtitle DESIGN AND CONSTRUCTION OF BONDED CONCRETE OVERLAYS				5. Report Date January 1991	
				6. Performing Organization Code	
7. Author(s) Willem A. van Metzinger, James R. Lundy, B. Frank McCullough, and David W. Fowler				8. Performing Organization Report No. Research Report 1205-4F	
9. Performing Organization Name and Address Center for Transportation Research The University of Texas at Austin Austin, Texas 78712-1075				10. Work Unit No. (TRIS)	
				11. Contract or Grant No. Rsch. Study 3/11-8-89/0-1205	
12. Sponsoring Agency Name and Address Texas Department of Transportation (formerly State Department of Highways and Public Transportation) P. O. Box 5051 Austin, Texas 78763-5051				13. Type of Report and Period Covered Final	
				14. Sponsoring Agency Code	
15. Supplementary Notes Study conducted in cooperation with the U. S. Department of Transportation, Federal Highway Administration Research Study Title: "Finite-Element Analysis of Bonded Concrete Overlays"					
16. Abstract This report summarizes studies of the performance of bonded concrete overlays (BCO), develops information on the failure mechanism of BCO, and documents an improved design model for BCO. Three pavements that received BCO placed in Houston, Texas, were closely observed, and the performance of these pavements was studied. The oldest of these pavements was about seven years, and performance information on the older BCO pavements was used not only in the development of a design model but also in suggested specifications that were adopted in the construction of the third BCO. The study of the failure mechanism examined the mechanisms that cause delamination and cracking. This study of the failure mechanism permitted the development of a design procedure through the use of a finite-element program.					
17. Key Words performance, bonded concrete overlays (BCO), failure mechanism, design model, pavements, specifications, construction, finite-element program			18. Distribution Statement No restrictions. This document is available to the public through the National Technical Information Service, Springfield, Virginia 22161.		
19. Security Classif. (of this report) Unclassified		20. Security Classif. (of this page) Unclassified		21. No. of Pages 52	22. Price

DESIGN AND CONSTRUCTION OF BONDED CONCRETE OVERLAYS

by

Willem A. van Metzinger
James R. Lundy
B. Frank McCullough
David W. Fowler

Research Report Number 1205-4F

Research Project 3/11-8-89/0-1205

Finite-Element Analysis of Bonded Concrete Overlays

conducted for

**Texas State Department of Highways
and Public Transportation**

in cooperation with the

**U. S. Department of Transportation
Federal Highway Administration**

by the

CENTER FOR TRANSPORTATION RESEARCH

Bureau of Engineering Research

THE UNIVERSITY OF TEXAS AT AUSTIN

January 1991

NOT INTENDED FOR CONSTRUCTION,
PERMIT, OR BIDDING PURPOSES

B. Frank McCullough, P.E. (Texas No. 19914)
David W. Fowler, P.E. (Texas No. 27859)

Research Supervisors

The contents of this report reflect the views of the authors, who are responsible for the facts and the accuracy of the data presented herein. The contents do not necessarily reflect the official views or policies of the Federal Highway Administration or the State Department of Highways and Public Transportation. This report does not constitute a standard, specification, or regulation.

There was no invention or discovery conceived or first actually reduced to practice in the course of or under this contract, including any art, method, process, machine, manufacture, design or composition of matter, or any new and useful improvement thereof, or any variety of plant which is or may be patentable under the patent laws of the United States of America or any foreign country.

PREFACE

Even though asphaltic concrete overlays on portland cement (PC) concrete have been used for some time, the use of bonded concrete overlays is relatively new in Texas. At the time of this report, bonded concrete overlays (BCO) had not been used on jointed concrete in Texas but had been placed only on continuously reinforced concrete paving. Because of this lack of experience, it became important to develop information on this type of rehabilitation. This report includes performance evaluations of BCO placed in Houston; studies stress development in BCO due to environmental stress as well as traffic loading; discusses the development of an empirical-

mechanistic design procedure for bonded concrete overlays on continuously reinforced concrete pavements; and identifies construction parameters important during the early age of the pavement. As the bonded concrete overlays were placed on the continuously reinforced concrete, the construction included several experimental features. Therefore, the performance evaluations included observations of BCO containing different aggregate types, grout or no grout, different types of reinforcing, different surface treatments of the existing pavement, and various types of bonding agents.

LIST OF REPORTS

Research Report 1205-1, "An Empirical-Mechanistic Design Method Using Bonded Concrete Overlays for the Rehabilitation of Pavements," by Willem A. van Metzinger, B. Frank McCullough, and David W. Fowler, presents the background and techniques used in developing a design model for bonded concrete overlays. January 1991.

Research Report 1205-2, "Delamination of Bonded Concrete Overlays at Early Ages," by James Ray Lundy, B. Frank McCullough, and David W. Fowler, presents a study of the delamination phenomena in bonded concrete overlays and suggests construction and material techniques to reduce delamination. January 1991.

Research Report 1205-3, "A Finite-Element Program for Analysis of Bonded Concrete Overlays," by C. V. G. Vallabhan, Mehmet Asik, and Khan Rahman, presents a finite-element program developed to study bonded concrete overlays subjected to thermal and surface loads. (Unpublished)

Research Report 1205-4F, "Design and Construction of Bonded Concrete Overlays," by Willem Van Metzinger, James R. Lundy, B. Frank McCullough, and David W. Fowler, presents an evaluation of the early-age performance of bonded concrete overlays and documents the development of a design model for bonded concrete overlays. January 1991.

ABSTRACT

This report summarizes studies of the performance of bonded concrete overlays (BCO), develops information on the failure mechanism of BCO, and documents an improved design model for BCO. Three pavements that received BCO placed in Houston, Texas, were closely observed, and the performance of these pavements was studied. The oldest of these pavements was about seven years, and performance information on the older BCO pavements

was used, not only in the development of a design model but also in suggested specifications that were adopted in the construction of the third BCO. The study of the failure mechanism examined the mechanisms that cause delamination and cracking. This study of the failure mechanism permitted the development of a design procedure through the use of a finite-element program.

SUMMARY

As the fourth and final report for this project, this report summarizes the previous three reports. The report evaluates the field performance of in-place bonded concrete overlays in Houston, Texas, evaluates a finite-element program, uses the finite-element program to model a bonded concrete overlay on continuously reinforced concrete paving, evaluates the environmental stresses in the overlay, and identifies construction control procedures which

may be used in specifications. Observations and analysis developed in this project indicate that delamination between the old and new material is a phenomenon which is probably an early-age problem associated with environmental loading. Observations also show that reinforcing type, thickness, and aggregate all influence transverse crack development, which relates to interface stresses at early ages.

IMPLEMENTATION STATEMENT

In this project, some consideration has been given to evaluating existing pavements to determine the feasibility of applying bonded concrete overlays. It is suggested that this technique be considered for use. The design system proposed in this study can

be used in the design of bonded concrete overlays on continuously reinforced concrete pavement. Several recommendations concerning construction control have also been offered, and these recommendations are suggested for use.

TABLE OF CONTENTS

PREFACE.....	iii
LIST OF REPORTS.....	iii
ABSTRACT.....	iii
SUMMARY.....	iv
IMPLEMENTATION STATEMENT.....	iv
CHAPTER 1. INTRODUCTION.....	1
1.1 Background.....	1
1.2 Purpose of the Study.....	1
1.3 Scope of the Study.....	1
1.4 Scope of the Report.....	2
CHAPTER 2. ANALYSIS OF FIELD PERFORMANCE OF BONDED CONCRETE OVERLAYS IN HOUSTON, TEXAS	
2.1 Introduction.....	3
2.2 Delamination.....	3
2.2.1 Early-Age Analysis.....	3
2.2.2 Long-Term Analysis.....	3
2.3 Transverse Cracking.....	6
2.3.1 Analysis of Each Survey.....	7
2.3.2 Student t-Tests of Differences Between Surveys.....	7
2.3.3 Analysis Without Direction and Lane.....	8
2.3.4 Analysis of Delaminated Areas.....	8
2.3.5 Analysis of Non-Delaminated Areas.....	9
2.3.6 Conclusions.....	9
2.4 Longitudinal Cracking.....	10
2.5 Conclusions.....	11
CHAPTER 3. MODELING OF BCO USING FINITE-ELEMENT METHOD	
3.1 Introduction.....	12
3.2 Methodology.....	12
3.3 Input Variables.....	13
3.4 Conclusions.....	13
CHAPTER 4. ANALYSIS OF WHEEL AND ENVIRONMENTAL STRESSES IN BONDED CONCRETE OVERLAY SYSTEMS	
4.1 Introduction.....	15
4.2 Early-Age Evaluation of BCO.....	15
4.2.1 Thermal Stresses.....	15
4.2.2 Influence of Shrinkage.....	15

4.3	Long-Term Evaluation of BCO.....	20
4.3.1	Traffic Loads.....	20
4.3.2	Environmental Stresses in BCO.....	23
4.4	Conclusions.....	24
CHAPTER 5. DEVELOPMENT OF AN EMPIRICAL-MECHANISTIC DESIGN METHOD FOR BCO		
5.1	Introduction.....	25
5.2	Failure Mechanisms.....	25
5.2.1	Punchouts in Delaminated Areas.....	26
5.2.2	Non-Reflective Cracking Areas.....	26
5.2.3	Reflective Cracking Areas.....	27
5.3	BCO Construction Criteria.....	27
5.4	Thickness Design.....	30
5.5	Long-Term Performance Prediction Model.....	32
5.6	Conclusions.....	33
CHAPTER 6. CONSTRUCTION CONTROLS		
6.1	Design.....	34
6.1.1	Thickness.....	34
6.1.2	Reinforcement.....	35
6.2	Specification.....	36
6.2.1	Materials.....	36
6.2.2	Surface Preparation.....	37
6.3	Construction.....	38
6.3.1	Environmental Controls.....	38
6.3.2	Bonding Agents.....	40
6.3.3	Curing.....	40
6.4	Summary.....	41
CHAPTER 7. CASE STUDY		
7.1	Design of BCO for the South Loop of IH-610, Houston.....	42
7.2	Construction Controls for the South Loop of IH-610, Houston.....	43
CHAPTER 8. CONCLUSIONS AND RECOMMENDATIONS FOR FUTURE WORK		
8.1	Conclusions.....	44
8.2	Recommendations.....	44
8.3	Recommendations for Future Work.....	44
REFERENCES.....		45

CHAPTER 1. INTRODUCTION

1.1 BACKGROUND

In the United States, many sections of the Interstate highway system are nearing the end of their design lives. The structural and functional capability of these highways can be improved by either ongoing maintenance, rehabilitation, or reconstruction. Rehabilitation has become an important factor in the Interstate system because it improves riding quality as well as structural capacity at a lower cost than reconstruction. When properly implemented, rehabilitation is also more permanent and effective than routine maintenance. The Interstate system consists of various types of pavement structures. Some are flexible pavements, where asphalt concrete is normally the wearing surface, while others are rigid pavements, where the surface layer is portland cement concrete. This study is mainly concerned with portland cement concrete pavement rehabilitation, specifically bonded concrete overlays (BCO) on existing continuously reinforced portland cement concrete pavements.

Various concrete overlay design procedures are available for engineers to use. Most of these design procedures are based on the Corps of Engineers Design Procedure. This procedure was mainly developed for overlays of airport pavement structures, which differ considerably in size and type of loading from highway overlays. Two main factors need to be considered when overlays are designed for highway applications. The first is the design system used to obtain an overlay thickness. The second factor is establishing how long the overlaid system will last. Current procedures give some indication based on limited empirical results.

In order to evaluate the long-term performance of the pavement structure, the failure mechanism should be known. This failure mechanism can then aid in understanding the problems associated with design and construction practices. The two main distress modes associated with BCO are cracking and delamination. The accepted cracking mechanism of overlays is based on empirical results or engineering judgment. Bonded concrete overlays are meant to produce reflective cracking that will coincide with the cracks in the existing pavement. This, however, does not always happen. Experimental bonded concrete overlay sections under surveillance in

Houston did not always provide reflective cracking. The currently assumed mechanism of crack formation is, therefore, not always applicable. Another field observation that influenced the long-term performance of bonded concrete overlays was the detection of delamination, as well as punchouts, occurring in overlaid structures on IH 610 in Houston. Cracking and delamination are, therefore, important parameters that should be investigated and controlled in the design and construction of bonded concrete overlays.

The above paragraphs have shown the status of bonded concrete overlays in the Interstate system and also some of the problems with the design of bonded concrete overlays.

1.2 PURPOSE OF THE STUDY

The main purpose of the study was to evaluate the early-age performance of and to develop a design model for bonded concrete overlays. The study involves characterizing failure mechanisms that cause delamination and cracking in bonded concrete overlays. By establishing the failure mechanisms, a design procedure can be developed to improve current design procedures as well as to improve the prediction of long-term performance of bonded concrete overlaid systems. Construction specifications can be developed from the early-age analysis to improve the long-term performance of BCO.

1.3 SCOPE OF THE STUDY

The objective of this study was to investigate BCO failures observed on pavements on the North Loop and the South Loop of IH-610 in Houston. Field observations were made, surveys were conducted, and the data were used to model BCO. A finite-element method (FEM) program was developed to model the behavior of BCO during early ages as well as the influence of wheel and environmental loading at later ages. Stress equations were developed for the design of overlay thickness. The equations were also used to develop criteria for selecting BCO as a rehabilitation method. Construction controls were developed from the

early-age analysis to be used in specifications for construction of BCO. The design method and construction controls were used in an example to illustrate the procedures developed. Finally, some conclusions and recommendations are made.

The specific objectives were:

- (1) to model phenomena observed on overlays in Houston, with specific reference to cracking behavior and delamination;
- (2) to accurately analyze the behavior of bonded concrete overlays at early ages, as well as to analyze the overlay after it is opened to traffic;
- (3) to develop a rational method for establishing when a BCO should be placed in favor of reconstruction or unbonded overlays;
- (4) to develop an easily usable design procedure for bonded concrete overlays incorporating the above factors; and
- (5) to develop construction controls for specifications.

1.4 SCOPE OF THE REPORT

Chapter 1 discusses the background, purpose, and scope of the report.

Chapter 2 evaluates the field performance of BCO in Houston, looking at early-age performance as well as long-term performance with specific attention to delamination and cracking.

Chapter 3 evaluates an FEM program which was used to model a BCO placed on a continuously reinforced concrete pavement.

Chapter 4 evaluates stress development in BCO as a result of environmental stress during the early ages as well as that resulting from traffic and environmental stresses at later stages.

Chapter 5 discusses the development of an empirical-mechanistic design procedure for BCO. A design procedure for BCO, as well as a long-term performance prediction model, is proposed.

Chapter 6 identifies construction control parameters that are important in the development of BCO during the early stages of its life.

Chapter 7 discusses a case study that illustrates the design procedure and defines construction controls for a section placed on the South Loop in Houston.

Chapter 8 discusses conclusions from this study and presents recommendations for future work.

CHAPTER 2. ANALYSIS OF FIELD PERFORMANCE OF BONDED CONCRETE OVERLAYS IN HOUSTON, TEXAS

2.1 INTRODUCTION

In order to evaluate the performance of the pavement, empirical data are needed to evaluate the long-term performance of bonded concrete overlays, and these data should be tied in with stress equations to complete a design model. Field data are normally very difficult to interpret, and the parameters necessary to explain the variability are not obtained in every case. However, the field data are normally the only means for establishing the long-term performance of a pavement. Furthermore, field data show types of failures which can then be modeled. These models can then be used to improve the design procedure and construction specifications. The data in this analysis were obtained from surveys done on Loop IH-610 North and South in Houston.

Survey procedures done on test sections in Houston include a visual condition survey to establish the (1) longitudinal crack length, (2) number of transverse cracks, and (3) extent of delamination. Transverse and longitudinal cracks were recorded on paper; from these notations the number of cracks and the lengths were obtained. Delamination was detected using sounding techniques. On test sections in Houston, reinforcing bars were used to "sound" the pavement. The bars were dropped from about 6 inches above the pavement surface. A solid sound indicated a non-delaminated area, while a hollow sound indicated a delaminated area.

Figure 2.1 shows a layout of the Houston area, indicating the test sections surveyed. The surveys were also normally accompanied by falling weight deflectometer readings at various intervals. The falling weight deflectometer readings give an indication of the modulus values of the different layers in the system.

2.2 DELAMINATION

Delamination of bonded concrete overlays in Texas was first noticed on Loop IH-610 North in March 1987. Condition surveys were conducted on the inside two lanes in both directions. The time at which the delamination took place was uncertain, because while it was detected several months after

construction, no sounding tests were done between the time of construction and March 1987. On the 2-inch and 3-inch sections on the South Loop, delamination was detected on the two inside lanes. Only a very small percentage of delamination was reported, and, again, the sounding survey did not occur until several years after placement. The question, then, is whether delamination is a progressive failure of bonded concrete overlays which can ultimately lead to total failure, or whether it is an early age phenomenon which is not progressive but which may increase the required maintenance on the overlay.

2.2.1 Early-Age Analysis

Other researchers have reported that delamination occurs early in the life of the overlay. Corroboration of this information came about through early observations of a bonded overlay placed on Loop IH 610 South. Researchers from the Center for Transportation Research were on site during the construction of several test sections that were included in the 5.5-mile bonded overlay project. Delaminated areas were discovered within 24 hours after placement in two of the test sections. Before trafficking, the debonding had progressed to encompass nearly 50 percent of the overlay in some test sections. The progression of the delamination can be seen in Figure 2.2. These two sections were eventually removed and replaced.

Delamination of the Loop IH 610 South test sections was always located adjacent to a joint or crack. This can be seen in the schematic of one of the sections shown in Figure 2.3. A similar pattern of delamination was found in debonded areas on the Loop IH-610 North.

2.2.2 Long-Term Analysis

The purpose of the long-term analysis is to compare three successive delamination surveys on the North Loop and establish whether the delamination was progressive. This will aid in establishing the significance of delamination in long-term performance of bonded concrete overlays. The data obtained from surveys were the time and traffic loadings since construction, aggregate type (siliceous river gravel or

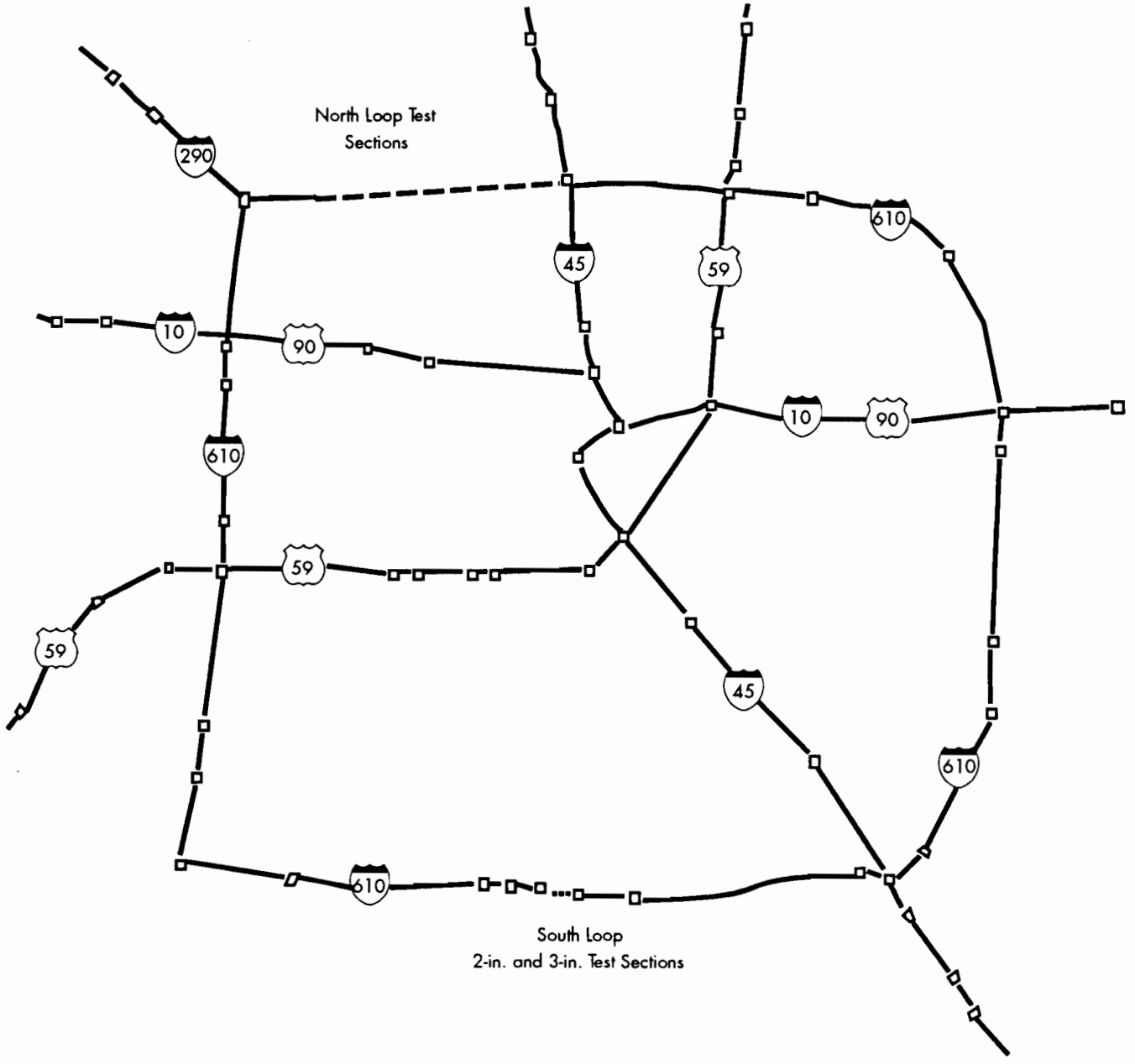


Figure 2.1 Test sections surveyed in Houston on the North and South Loops of Interstate Highway 610

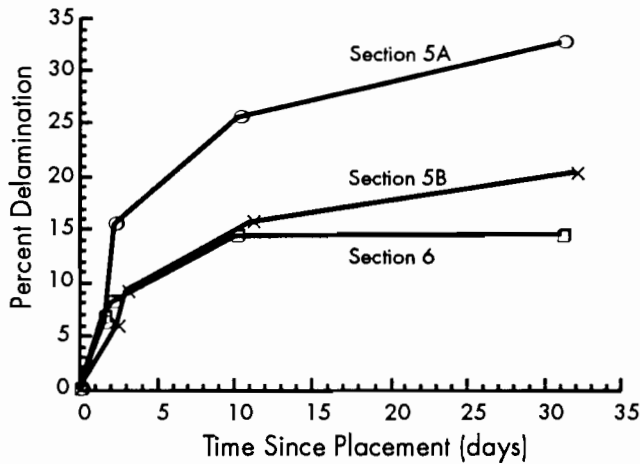


Figure 2.2 Progression of delamination in those test sections with debonding

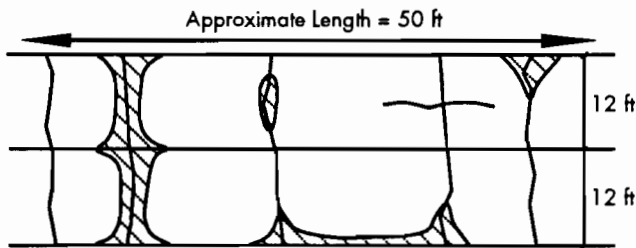


Figure 2.3 Schematic of test section showing typical location of debonding

limestone), grout or no grout, type of reinforcement (wire or fiber), direction (east or west), lane, and temperature differential between the air temperature at the time of placement and the lowest temperature during the first night following the day of construction. Fourteen lane-miles were divided into 100-foot analysis sections.

2.2.2.1 Analysis of Each Year

Figure 2.4 shows the average percent delamination along the length of the project for the three different surveys. It can be seen from the figure that the

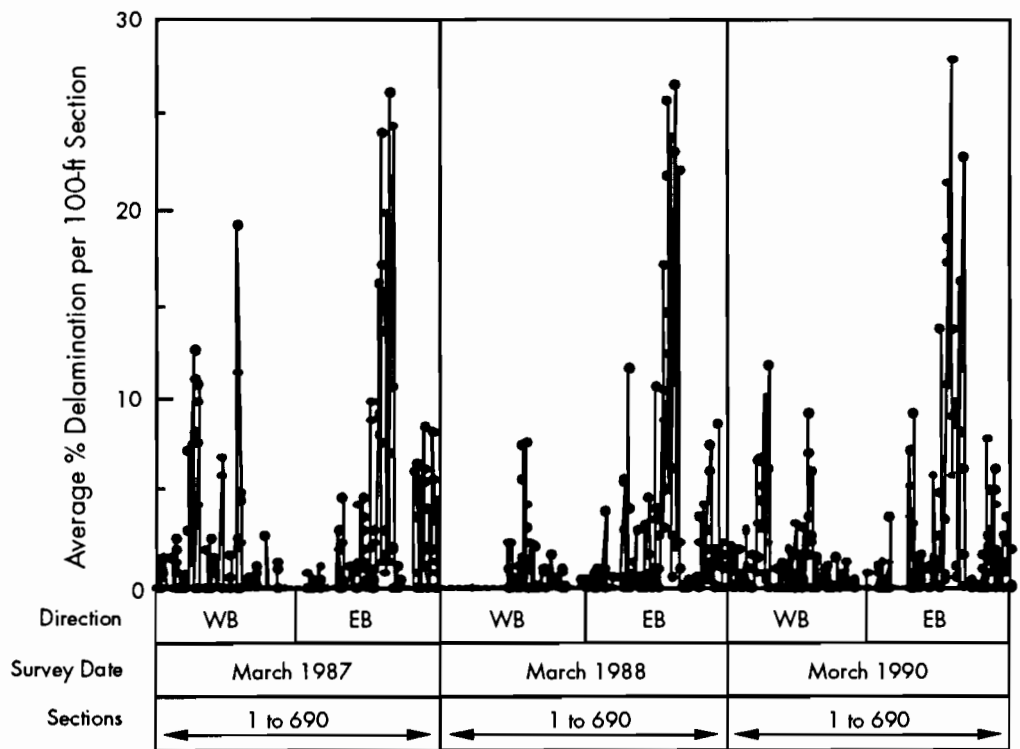


Figure 2.4 Delamination survey results for each of the three years

same trends exist for each survey. An analysis of variance was completed for each survey year separately. The results showed that aggregate type was significant in each year and that for the 1990 survey, the direction and lane interaction were also significant. This means that a significant amount of the variability in the model is described by the aggregate type. Siliceous river gravel (SRG) experienced higher delamination than the limestone (LS). However, about 85 percent of the project was constructed using siliceous river gravel (SRG) aggregate. The SRG overlay was therefore exposed to a much wider range of conditions than the LS overlay.

The time of placement varied and, therefore, the environmental factors could have had considerable influence on the fact that SRG showed much higher delamination. However, it can be concluded only that there was a difference in delamination between SRG and limestone for the test sections surveyed.

2.2.2.2 Analysis of Full Factorial

An analysis of the full factorial was completed and provided two interactions that were significant: the interaction of direction with traffic and direction with time. The conceptual model for this analysis is:

$$\% \text{ Delamination} = f\{\text{Traffic} \times \text{Direction}, \text{Time} \times \text{Direction}\}.$$

Figures 2.5 and 2.6 (page 6) show the average percentage of delamination by direction and time,

and direction and traffic, respectively. The time levels selected were 6 to 24 months as low, 25 to 42 months as medium, and 43 to 54 months as high. The traffic levels selected were 0 to 500,000 ESAL as low, 500,000 to 900,000 ESAL as medium, and 900,000 to 1,600,000 ESAL as high.

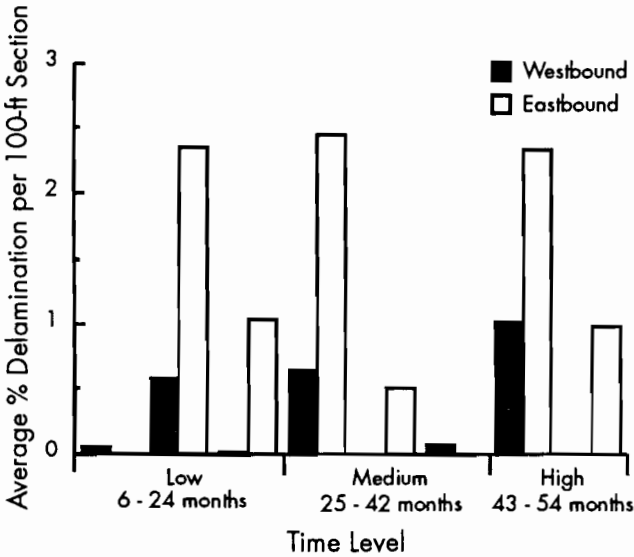


Figure 2.5 Interaction of direction and time since placement

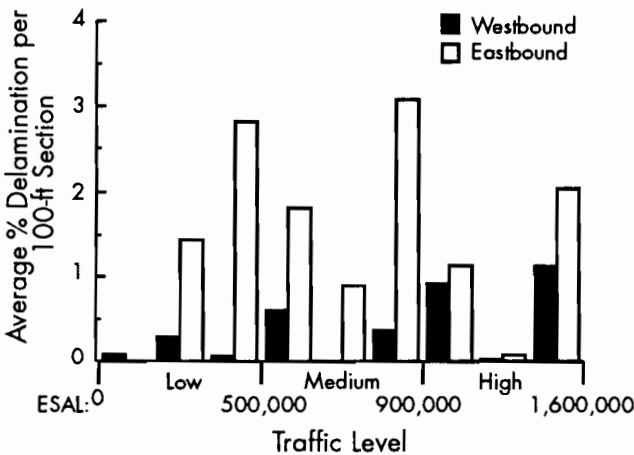


Figure 2.6 Interaction of direction and traffic

It is evident from these two figures that no real trend exists between delamination and traffic or time, but that the directional factor is very important. The data obtained from both the east and west directions were constructed over a variety of conditions.

Table 2.1 shows an analysis of variance of only the main effects. It shows that the direction, reinforcing, aggregate, and temperature differences between temperature at placement and minimum temperature during the first night after placement are all significant. The conceptual model is:

$$\% \text{ Delamination} = f\{\text{Direction, Reinforcing, Aggregate, Temperature Differential}\}.$$

2.2.2.3 T-Test and Analysis of Variance

Student t-tests between the percent delamination of March 1988 versus March 1987, March 1990 versus March 1987, and March 1990 versus March 1988 were run, and no significant differences were found between any of these. The results of the t-tests are shown in Table 2.2.

Table 2.2, together with the conceptual model shown in the previous section, implies that delamination is not progressive in this project and that early-age variables, of which temperature difference is an indicator, are important. It is, therefore, concluded that delamination is an early-age phenomenon.

2.2.2.4 Conclusions

It can, therefore, be concluded that delamination of bonded concrete overlays is an early-age problem that probably occurs during the first few weeks after construction. Delamination is not progressive, but its influence on the long-term performance of the pavement is uncertain, and delaminated areas may ultimately need maintenance before areas that are not delaminated.

2.3 TRANSVERSE CRACKING

It is generally assumed that transverse cracks reflect through the BCO after placement. However, an investigation of 2- and 3-inch BCO test sections showed that this is not always the case. These sections were constructed on an 8-inch CRC pavement located on Loop IH 610 South (see Figure 2.1). Factors investigated were reinforcement and thickness. The combination shown in Table 2.3 was constructed in 1983. Wire-reinforced sections were reinforced with the same percentage reinforcing as the existing pavement section, and the concrete was expected to react in the same way as the original pavement did. This increases the probability of reflective cracking, as is evidenced by Table 2.3, in which the average crack spacings between before- and after-overlay data are not significantly different. Fiber-reinforced concrete is a different material, resulting in a significantly different average crack spacing.

The North Loop data are evaluated by dividing the analysis into an annual analysis, a combined analysis with all variables, and, finally, an analysis without direction and lane, to evaluate the progression of increase in the number of cracks per 100-foot section.

Table 2.1 Analysis of variance for delamination

Source	DF	Sum of Square	Mean Square	F-Value	PR > F
Model	8	1,580	197	25.4	0.0001
Error	1,911	14,856	8		
Corrected Total	1,919	16,436			

Source	DF	Sum of Square	F-Value	PR > F	Significant
Direction	1	822.196	105.76	0.0001	Yes
Lane	1	0.074	0.01	0.9220	No
Reinforcing	1	270.865	47.71	0.0001	Yes
Aggregate	1	240.696	30.96	0.0001	Yes
Grout	1	16.149	2.08	0.1497	No
Traffic	1	22.565	2.90	0.0886	No
Time	1	19.143	2.46	0.1168	No
Temp Difference	1	81.934	10.54	0.0012	Yes

Table 2.2 T-test analysis of differences = 0

Comparison	Mean	Std Error	T	Prob > T	Significant
Delamination 1988 – Delamination 1987	0.0071	0.0647	0.1096	0.9128	No
Delamination 1990 – Delamination 1987	0.0634	0.0841	0.7532	0.4516	No
Delamination 1990 – Delamination 1988	0.0687	0.0923	0.7444	0.4570	No

Table 2.3 Before- and after-overlay average crack spacing

Section	Avg Before-Overlay Crack Spacing (ft)	Avg After-Overlay Crack Spacing (ft)
2-in. Nonreinforced	2.3	3.0
2-in. Reinforced	1.8	1.4
3-in. Reinforced	2.3	2.7
3-in. Fiber Reinforced	2.4	10.9
2-in. Fiber Reinforced	4.9	45.7

After-overlay crack spacings were calculated as the average of November 1984 and April 1990 crack spacings due to no statistical difference between the two.

2.3.1 Analysis of Each Survey

In an analysis of variance study of each survey, the most important parameter obtained from the analysis is the aggregate type which was significant in all three years. This suggests that the initial crack development depends on the aggregate type used. This pattern of crack development is very similar to that of newly constructed, continuously reinforced concrete pavements. In general, concrete made with siliceous river gravel shows more cracking than concrete made with limestone aggregate (Ref 1).

2.3.2 Student t-Tests of Differences Between Surveys

Comparison of t-tests for various years showed that no significant difference exists between March 1987 and March 1988 data. As can be seen from Table 2.4 (page 8), the analysis of 1990 data showed a significant increase above those of 1987 and 1988.

While this analysis indicates a significant increase in the number of transverse cracks in each section, it does not consider the influence of delamination on the development of cracking. An analysis must,

Table 2.4 Student t-test results to determine whether the number of transverse cracks is the same between surveys

Comparison	Mean	Std Error	T	Prob > T	Significant
TCracks 1988 – TCracks 1987	- 1.3084	0.6912	- 1.8930	0.0589	No
TCracks 1990 – TCracks 1987	5.5211	0.6016	9.1775	0.0001	Yes
TCracks 1990 – TCracks 1988	6.3913	0.6710	9.5244	0.0001	Yes

therefore, include the study of transverse cracks in delaminated versus non-delaminated areas as well as a comparison of the different analysis years.

2.3.3 Analysis Without Direction and Lane

The next step in the analysis was to model transverse cracking in delaminated and non-delaminated areas. Table 2.5 shows the analysis of variance (ANOVA) of only the main effects of transverse cracks without direction and lane. Significance exists in the reinforcing, aggregate, time, and temperature differential. A conceptual model for this analysis is:

$$\# \text{ Transverse Cracks} = f(\text{Reinforcing, Aggregate, Time, Temperature Differential}).$$

When the time is plotted against the number of transverse cracks, no real trend exists. In an analysis with interactions, the interaction of reinforcing with time was also significant. Twenty percent of the variability is explained, and a plot of the residuals versus predicted values of the model showed that the model explains the data sufficiently. It must then be assumed that factors not measured by these data are responsible for the rest of the variability in the development of the transverse cracks. The by-year analysis showed that the aggregate type is significant. It must, therefore, be assumed that the development of cracking is dependent on the aggregate type and reinforcing used in the pavement, which is the same conclusion made from the 2-inch and 3-inch test sections on the IH-610 South Loop.

The time factor is also significant and will give an indication of the development of transverse cracks with time. Figure 2.7 shows a plot of the average number of transverse cracks per 100-foot section versus the year of analysis. A student Newman-Keuls test was performed on the averages and showed that all three surveys are significantly different from each other. It can, therefore, be concluded that no real trend exists between the transverse cracks and year of analysis. This may be due to the variability associated with measurements and operators. Factors such as misalignment of analysis sections among the three different condition surveys can cause variability not explained by the model. During the 1988 and 1990 surveys, data were collected using a vehicle-mounted video camera traveling at approximately 50 mph. Analysis sections within the project were located by reference to the vehicular fifth-wheel and bridge ends. It is possible that some of the variability in the analysis can be assigned to the misalignment of the sections during data reductions. An analysis was also made of the delaminated and non-delaminated areas. These analyses are discussed in the next paragraphs.

2.3.4 Analysis of Delaminated Areas

The analysis showed that the aggregate type, the difference between the air temperature and lowest ambient temperature during the first night after placement, and an interaction between temperature difference and reinforcing are significant. This again suggests that the cracking in delaminated areas depends on the early-age factors and the aggregate

Table 2.5 ANOVA for transverse cracking excluding direction and lane

Source	DF	Sum of Square	Mean Square	F-Value	PR > F
Model	6	61,219	10,203	66.1	0.0001
Error	1,895	292,491	154		
Corrected Total	1,901	353,710			
Source	DF	Sum of Square	F-Value	PR > F	Significant
Reinforcing	1	32,179.12	208.48	0.0001	Yes
Aggregate	1	16,337.77	105.85	0.0001	Yes
Grout	1	4.59	0.03	0.8631	No
Traffic	1	200.49	1.30	0.2545	No
Time	1	2,687.02	17.41	0.0001	Yes
Temp Difference	1	6,107.22	39.57	0.0001	Yes

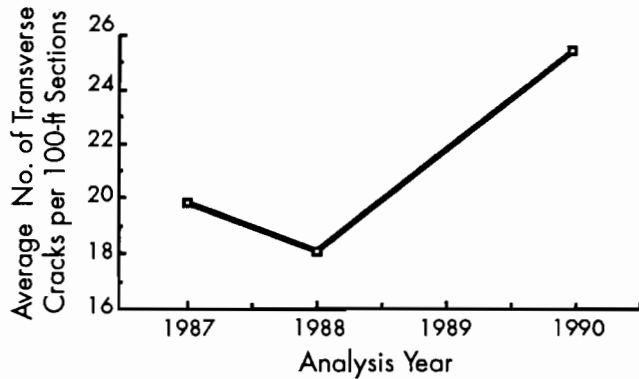


Figure 2.7 Average number of transverse cracks per 100-foot section for delaminated and non-delaminated areas

type. These are very much the same as the results of the by-year analysis completed previously. The model explains only 15 percent of the variability.

Figure 2.8 shows the average number of transverse cracks per section for delaminated sections. A student Newman-Keuls test was done to compare the means of each different survey year. This test showed a significant difference in transverse cracking between the 1990 and the 1987 and 1988 survey results. No significant difference was found between the 1987 and 1988 results. It can be seen from Figure 2.6 that an increasing trend exists between the number of transverse cracks and time. We can therefore conclude that transverse cracks increase significantly in delaminated areas. The development of this cracking will be discussed later when a stress analysis of delaminated pavements is made.

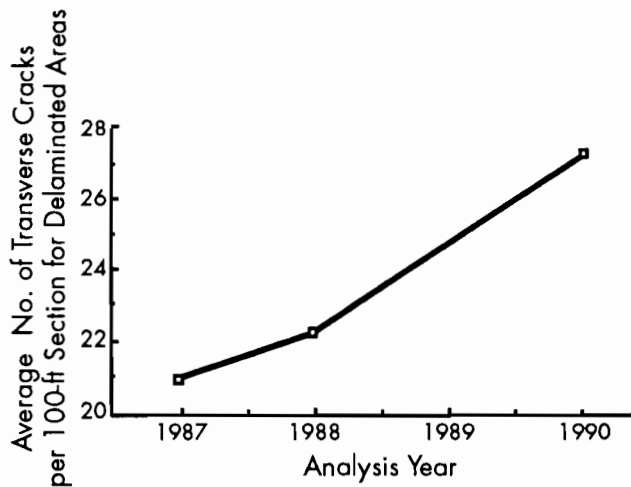


Figure 2.8 Average number of transverse cracks per 100-foot section for delaminated sections

2.3.5 Analysis of Non-Delaminated Areas

The same analysis procedure used for delaminated areas was used for non-delaminated areas. The conceptual model can be illustrated by the following equation:

$$\% \text{ Delamination} = f(\text{Aggregate, Analysis Year}).$$

Only the aggregate and analysis year were found to be significant. The aggregate was also significant for the by-year analysis, which again shows the difference in crack development for different aggregates. A student Newman-Keuls test was performed to compare the average number of transverse cracks per section for each year. It showed significant differences between all three years in which condition surveys were performed. Figure 2.9 shows a plot of the average number of cracks versus time of survey. It is evident that nothing constructive can be concluded from this information. Further surveys will be needed to evaluate any trend that may exist in the development of transverse cracks. These surveys should be conducted after a few years to see if the effect of traffic and time are significant or if these effects are important only in delaminated areas.

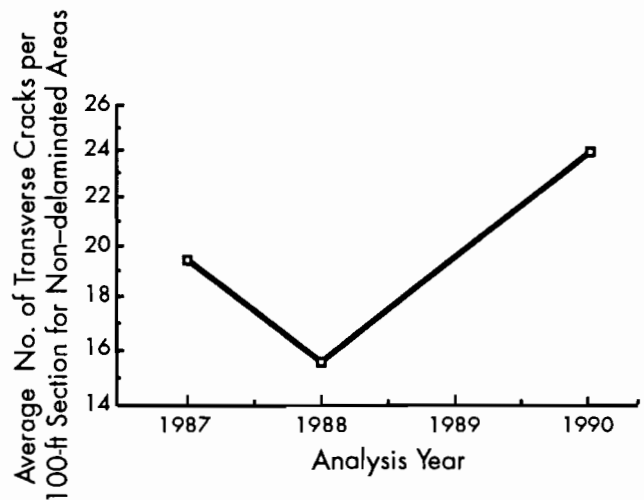


Figure 2.9 Average number of transverse cracks per 100-foot section for non-delaminated areas

The model describes 23 percent of the variability. Again, it can be concluded that factors not measured in these data are responsible for this low percentage.

2.3.6 Conclusions

Based on the analyses described above, it can be concluded that transverse cracks increase in delaminated areas, while no statistical evidence were found that transverse cracks increased in non-delaminated

areas. It is also concluded that further surveys are needed to evaluate the development of transverse cracks in non-delaminated areas and to further evaluate the trend that exists in non-delaminated areas.

2.4 LONGITUDINAL CRACKING

Longitudinal cracking data were obtained only during the March 1987 and March 1990 condition surveys. The same procedure used to evaluate transverse cracking is used to evaluate longitudinal cracking.

There is no significant difference in the length of longitudinal cracks between delaminated and non-delaminated areas. There is, however, significantly more longitudinal cracking in 1990 data than in 1987 data. An analysis of variance was performed with the time since placement variable included in the data. Twenty-six percent of the variance is explained in the model which uses the square root of the cracking. All the other variables are linear except traffic, which is modeled using the log of the traffic. The ANOVA table for an analysis of only main effects is shown in Table 2.6. The main effects—aggregate, traffic, temperature difference, and time—are significant. The conceptual model is:

$$\sqrt{\text{Length of longitudinal cracking}} = f(\text{aggregate, log(traffic), temperature difference, time})$$

The interactions of traffic and time, time and year, and traffic and year are also significant. It has been said before that there is much more longitudinal cracking in 1990 data than in 1987 data. Study of plots of longitudinal cracks versus traffic level and temperature difference showed no conclusive evidence of any trend.

Figure 2.10 shows a plot of traffic versus average length of longitudinal cracking. The same levels as

discussed before are used. It is evident from this figure that no real trend exists between traffic and longitudinal cracking. Residuals plotted against longitudinal cracking show an increasing linear relationship. Several models were evaluated, but variables other than those measured had an apparent influence on the development of longitudinal cracking.

Further compounding the problem is the lack of data concerning the sawcuts made at early age. Some areas may have been sawcut before cracking, while others were not. A longitudinal crack will develop and is part of this dataset, although some areas that were sawed and then cracked—after sawing and parallel to the crack—are not reflected in the data. It is, therefore, difficult to evaluate longitudinal cracking from the data available.

It can then be concluded that although the length of longitudinal cracking increased from 1987 to 1990, no evidence was found relating it to traffic or time. Although the traffic and time parameters

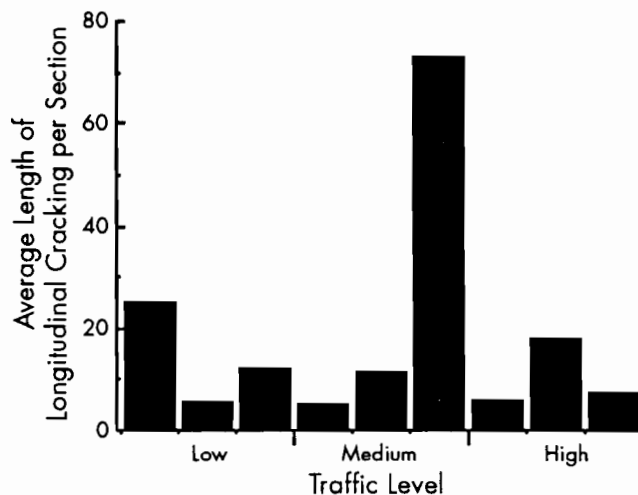


Figure 2.10 Average length of longitudinal cracking versus traffic

Table 2.6 ANOVA for longitudinal cracking without direction and lane

Source	DF	Sum of Square	Mean Square	F-Value	PR > F
Model	6	81,974.31	13,662.38	19.55	0.0001
Error	1,348	942,131.28	698.91		
Corrected Total	1,354	1,024,105.58			
Source	DF	Sum of Square	F-Value	PR > F	Significant
Reinforcing	1	15,700.08	22.46	0.0001	Yes
Aggregate	1	2,415.77	3.46	0.0632	No
Grout	1	1,973.06	2.82	0.0932	No
Traffic	1	7,435.11	10.64	0.0011	Yes
Time	1	15,834.18	22.66	0.0001	Yes
Temp Difference	1	48,220.44	68.99	0.0001	Yes

were found to be significant, no clear relationship could be isolated. The temperature difference was also found to be significant, but no conclusion can be made because there were no available data to indicate whether the pavement cracked before or after sawcutting.

2.5 CONCLUSIONS

This chapter evaluated the field performance of test sections under the surveillance of The University of Texas at Austin. The results from these analyses will be used with the computer analysis results to form the conceptual evaluation of a design system for bonded concrete overlays.

It appears that delamination of bonded concrete overlays is an early-age problem that occurs the first few weeks after construction. Delamination is not progressive over the period investigated, but the influence of delamination on the long-term performance of the pavement is uncertain. Intuitively, delaminated areas would require maintenance before non-delaminated areas, which will have an economical impact.

It can further be concluded that reinforcing type, thickness, and aggregate are important in transverse crack development in bonded concrete overlays. Different reinforcing procedures produce different crack spacings. Wire-reinforced sections show smaller crack spacings than do fiber-reinforced sections. Also, transverse cracks increase in delaminated areas while no statistical evidence was found that transverse cracks increased in non-delaminated areas. Furthermore, additional surveys are needed to evaluate the development of transverse cracks in non-delaminated areas and to evaluate the trend which exists in these areas.

It can be concluded that although the length of longitudinal cracking increased from 1987 to 1990, no evidence was found relating it to traffic or time. Although these parameters were found to be significant, no relationship could be found. The temperature difference was also found to be significant, but a conclusion cannot be made because no data indicated whether the pavement cracked before or after sawcutting. The sections on the South Loop showed that reinforcing significantly influences the formation of longitudinal cracking, which is also influenced by environmental factors, specifically during construction.

Finally, it should be remembered that although traffic did not show any significance in longitudinal or transverse cracking development, the overlays analyzed are only as much as seven years old. However, as the pavement ages, fatigue cracking will become more apparent in the analysis.

The information obtained from the evaluation of the field performance of BCO can be conceptually illustrated using the following equations:

$$\# \text{ Transverse Cracks} = f\{\text{Reinforcing, Aggregate, Thickness, Time, Temperature Differential}\}$$

$$\text{Length of Longitudinal Cracks} = f\{\text{Reinforcing, Temperature Differential}\}$$

$$\% \text{ Delamination} = f\{\text{Aggregate, Temperature Differential}\}.$$

With these conclusions in mind, the conceptual philosophy can be formed, together with a computer analysis of the pavement for a design system for bonded concrete overlays, which is discussed in the next chapter.

CHAPTER 3. MODELING OF BCO USING FINITE-ELEMENT METHOD

3.1 INTRODUCTION

In Chapter 2, field observations were analyzed and discussed. Two important observations were made. The first is that delamination occurs at early ages and, based on the experience in Houston, is not progressive. The second is that transverse cracking of bonded overlays is not always reflective. In order to further evaluate the mechanism of delamination and the long-term failure mechanism of the BCO, mechanistic procedures are needed to model the behavior observed in the field and to correlate the model with field performance. A finite-element method (FEM) was, therefore, developed at Texas Tech University in conjunction with the Center for Transportation Research (Ref 8). The purpose of this chapter is to discuss the development and use of the FEM program to model BCO according to the field observations discussed in the previous chapter.

3.2 METHODOLOGY

A two-dimensional FEM program was developed. Eight-noded quadrilateral two-dimensional plane strain elements are used as the basis of the program. Plane strain or stress problems can be evaluated using the program. For thermal stress evaluation of concrete pavements, the plane strain analysis provides realistic answers.

Wheel loading is an axi-symmetric, or three-dimensional, analysis problem and, therefore, the two-dimensional program cannot be used directly for wheel loading. By reducing the applied load, or increasing the width of the analysis section, the stress values obtained can be correlated with the Westergaard equation or with other three-dimensional programs such as ILLISLAB. The correlation can then be used to get equivalent loads for a standardized load that will produce the same stress values as the Westergaard equation. A major assumption in this procedure is that the cracking and possible delamination is assumed to act in a two-dimensional plane.

A special feature introduced into the program is horizontal and vertical slip elements, as well as the ability to model reinforcing bars. The slip element

consists of 4-noded nonlinear elements, with no thickness. The reinforcing is modeled using 3-noded linear strain bar elements. The slip elements are used to model the interface between the existing pavement and the overlay, as well as the slip plane between the existing pavement and the subbase. The slip elements can further be used to model cracking in the pavement. The bar elements are used to model reinforcing in the existing pavement as well as in the overlay. Figure 3.1 shows a section through a pavement system showing the layers modeled with the FEM program. The 8-noded elements are shown with four layers, where Layer 1 is the overlay, Layer 2 is the existing pavement, Layer 3 is the subbase, and Layer 4 is the roadbed.

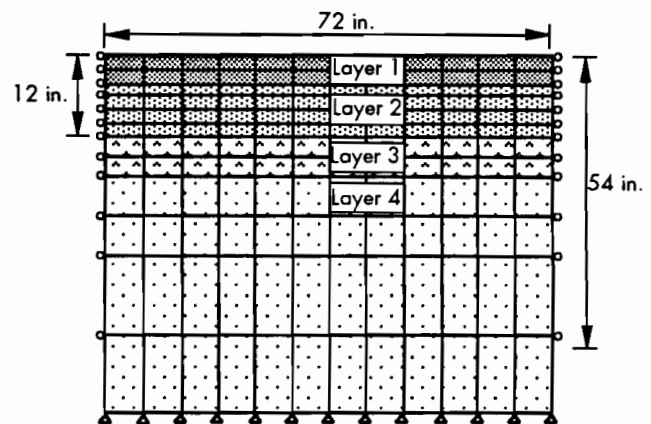


Figure 3.1 Layers and eight-noded elements for FEM program analysis

Figure 3.2 shows the slip element layout as modeled in the FEM program. Potential delamination zones are modeled as horizontal slip lines, while the cracks and potential cracks are modeled using vertical slip elements. The reinforcing bars can be modeled by introducing bar elements between two layers of horizontal 8-noded elements. Bar elements cannot be placed next to a slip element due to the configuration of a 4-noded slip element versus a 3-noded bar element. Slip elements are given certain

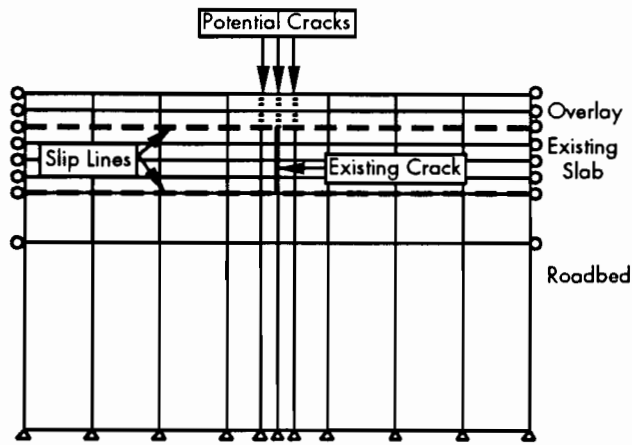


Figure 3.2 Layout showing positions of slip lines (horizontal slip elements) and potential and existing cracks (vertical slip elements)

properties and failure values that will be discussed later. The methodology used in the program is that, for a certain type of loading, deflections are calculated and from that stresses are obtained. The shear and tensile stress of the slip elements are compared to the corresponding strength. If the strength of a slip element is less than the stress, the slip element will break loose. The deflections and stresses are calculated for the "new" system and again strengths and stresses are compared. The iteration process will carry on until equilibrium is obtained. The deflections and stresses for the system when it is in equilibrium are then printed.

The finite-element method program can, therefore, be used to evaluate an analysis factorial to establish stress equations that include the variables influencing the early-age and long-term performance of an overlaid system. Furthermore, the influence of delamination, the effect of the condition of the existing system at the time the overlaid system is opened to traffic, and the remaining life of the existing pavement can be analyzed.

3.3 INPUT VARIABLES

Several input values are needed apart from the physical layout of the system to be analyzed. The inputs for each 8-noded element are the modulus of elasticity, Poisson ratio, width to be analyzed, and coefficient of thermal expansion. The use of the slip elements requires knowledge of the stress-deformation relationship between two adjoining elements. Figure 3.3 shows the general form of the relationship assumed between shear and tensile stress and deformation. Specific inputs include the maximum allowable stress and the slope of the stress-deformation curve. Bar elements require the

input of the modulus of elasticity of the reinforcing, the cross-sectional area, and the coefficient of thermal expansion. Loading may consist of thermal or wheel loadings, deflections, or a combination of the three.

Most of the input variables are easily obtainable from literature. The stress-deformation relationship of the slip elements is not easily obtainable because of the brittleness of concrete as well as the lack of data establishing such a ratio. However, based on a literature review and selected testing at The University of Texas at Austin, reasonable values were chosen.

3.4 CONCLUSIONS

Work by van Metzinger (Ref 3) concluded that certain assumptions must be made before using the program. First, as discussed before, the program was developed to evaluate plane strain problems. The actual wheel load stresses in a concrete pavement system are an axi-symmetric problem. Therefore, the assumption is made that, by increasing the section analysis width or reducing the load used in the analysis, a stress similar to that obtained using Westergaard analysis can be determined. Inherent in this is the assumption that the Westergaard analyses are applicable and comparable to elastic layered theory.

A further assumption is that the pavement will actually respond to cracking in a manner similar to that observed in the two-dimensional program, even though the actual system is three-dimensional. It is therefore assumed that, although boundary conditions change due to cracking within the pavement system, the stresses obtained from a two-dimensional analysis are still true.

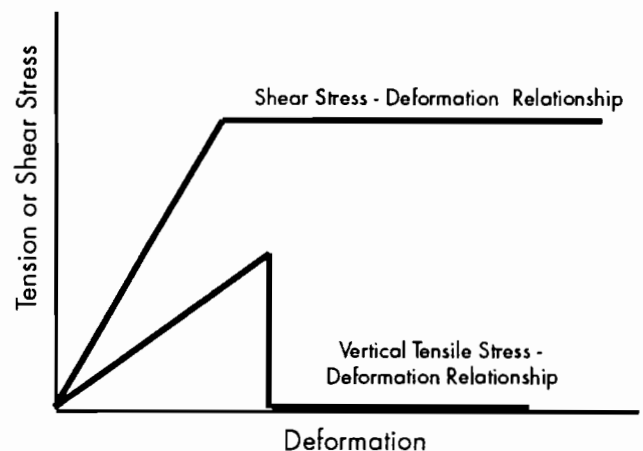


Figure 3.3 Stress-deformation relationship for slip elements

From the above paragraphs, it can be concluded that this analysis method does have certain limitations and uncertainties. The biggest limitation is that the program is a plane strain program used to calculate axi-symmetric stresses. Combining the wheel load stresses and environmental stresses will be done only with difficulty and some uncertainty.

Another limitation is that the method of incorporating cracking in the pavement system is limited. Cracking may occur in a meandering way and the percentage delamination may be higher at the edge

of the pavement than at the interior. These facts cannot be modeled using the finite-element program.

However, although these limitations exist and several assumptions had to be made in order to analyze the pavement in a cost-effective manner, it is concluded that the stress development obtained from the analysis can be used to evaluate the early-age and long-term performance by applying it to the system, using good engineering judgment and correlations with field observations.

CHAPTER 4. ANALYSIS OF WHEEL AND ENVIRONMENTAL STRESSES IN BONDED CONCRETE OVERLAY SYSTEMS

4.1 INTRODUCTION

The purpose of this chapter is to evaluate the stresses in BCO and to model field behavior described previously. A related purpose of this chapter is to analyze the effects of imposed loadings and environmental conditions on an overlaid pavement structure and to assess the pavement response to these loadings. The results of this assessment will be used to develop a failure model for the system. The long-term performance of the overlaid pavement depends on the type of overlay and on the condition of the existing pavement. Long-term performance is also affected by the presence of debonding. Field observations have shown delamination to be an early-age phenomenon and, therefore, early-age characteristics of bonded overlays will be evaluated first.

4.2 EARLY-AGE EVALUATION OF BCO

The evaluation of bonded overlays at early ages is believed to be critical to understanding the formation of delamination in overlays. As noted earlier, debonding was located in a bonded overlay in Houston, Texas within 24 hours following placement. This, coupled with reports of early debonding from other agencies, prompted the investigation of bonded overlays at early ages. Of special concern was the role of temperature- and shrinkage-induced stresses in the development of delamination. The finite-element method program described in the previous sections was used to analyze the stresses at the interface of the overlay and base slab. Before these stresses can be analyzed, the temperature distribution in the pavement must be determined and the importance of early volume change due to shrinkage of the overlay concrete must be evaluated.

4.2.1 Thermal Stresses

Temperature distributions in recently overlaid slabs were estimated by adapting a technique developed by Fintel and Khan to describe the temperature distribution in a concrete member some time following placement. Temperature distributions

were determined for the extremes in season (summer and winter) and time of day (early morning and late afternoon). A complete description of the procedure used to determine the temperature distribution with depth 12 and 24 hours after placement is described in Ref 2. Typical distributions are shown in Figure 4.1 (page 16) for a summer morning placement.

Temperature distributions similar to those shown above were analyzed using the finite-element method program, NSLIP. These distributions were developed after assuming a maximum air temperature drop of 30 degrees during the first 24 hours. Results show that the maximum tensile and shear stresses occur at or near the interface between the overlay and the existing slab (see Figures 4.2 and 4.3, page 17). Overlay placement during winter mornings was identified as the critical combination of season and time of placement among those investigated.

As seen in Table 4.1 (page 18), the maximum shear stress for the winter morning placement was approximately 24 psi. This value of shear stress is low, and under most circumstances would not cause debonding of the overlay. However, at early ages (less than 48 hours), the interface shear strength is also low; therefore, at early ages these stresses may be sufficient to induce delamination. These stresses were calculated for an edge condition. The results of similar calculations completed for an interior condition near a crack showed higher stresses than did the edge condition, although again the winter morning temperature distribution produced the highest stresses. The maximum stress was approximately 30 psi, as shown in Table 4.2 (page 19). The importance of these stresses will be discussed as they pertain to construction controls.

4.2.2 Influence of Shrinkage

Investigation of the importance of early-age shrinkage was undertaken to determine if the volume changes that occurred in the first 24 to 48 hours after placement were of sufficient magnitude to cause debonding. Other investigators have researched the volume change phenomenon of concrete. Most of the research attempted to characterize

Summer Morning Placement
Air Temperature Differential =
30°F

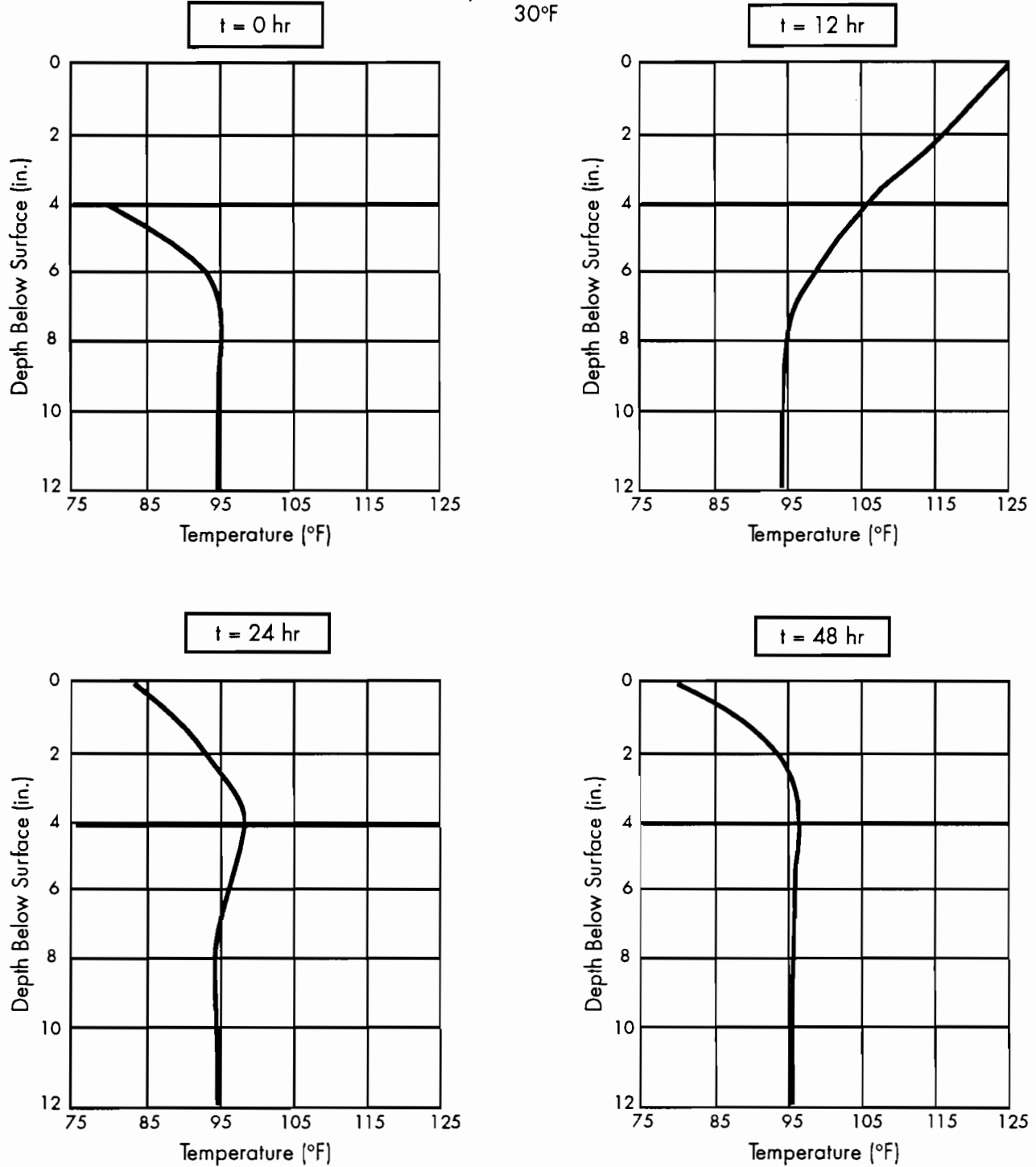


Figure 4.1 Temperature distribution in the pavement for a summer morning placement at 0, 12, 24, and 48 hours after placement of the overlay

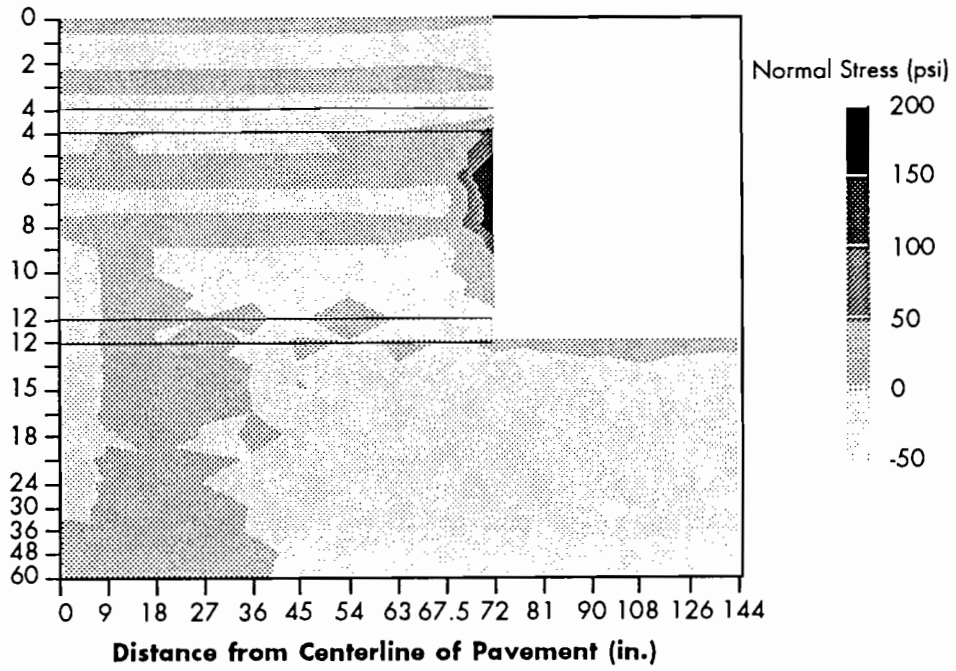


Figure 4.2 Normal stress contour for a 4-inch BCO on an 8-inch CRC pavement 24 hours after placement

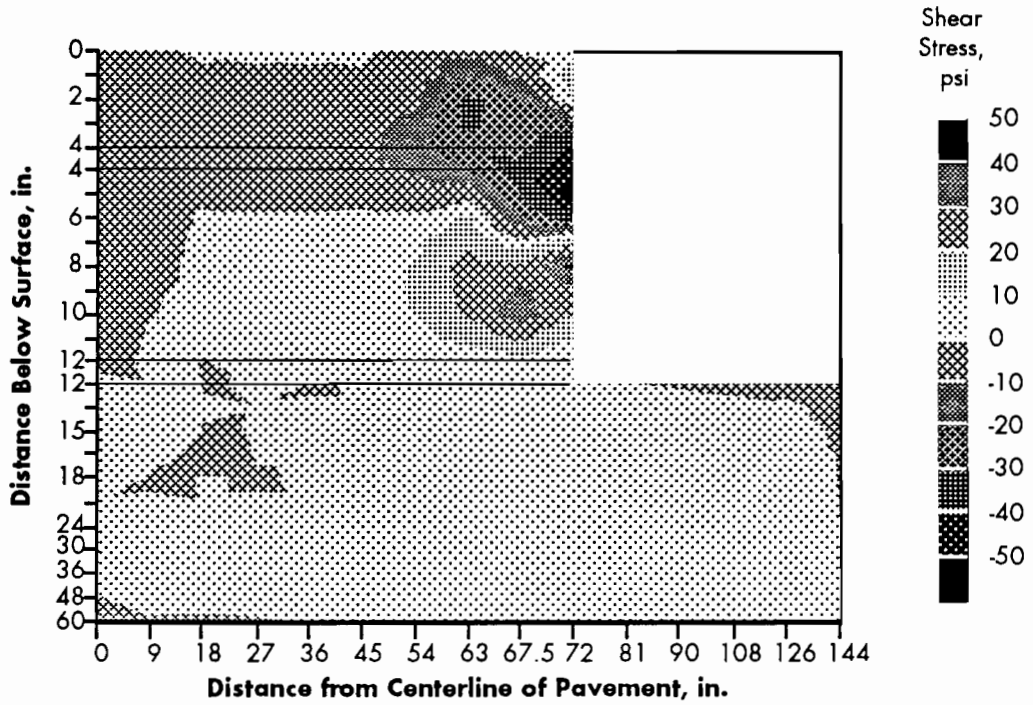


Figure 4.3 Shear stress contour for a 4-inch BCO on an 8-inch CRC pavement 24 hours after placement

Table 4.1 Maximum shear and normal stresses calculated for the edge condition

Season of Placement	Time of Placement	Time of Analysis	Overlay Thickness (in.)	Overlay Coeff.	Slab Modulus	Overlay Modulus	Winter								Summer										
							6 AM				6 PM				6 AM				6 PM						
							12 hrs		24 hrs		12 hrs		24 hrs		12 hrs		24 hrs		12 hrs		24 hrs				
							2	4	2	4	2	4	2	4	2	4	2	4	2	4	2	4			
6,000	6	6	6	6	6	6	4.5	-7.8	-15.9	-22.0	-6.0	-5.3	8.2	-5.9	4.7	8.1	-14.5	-9.1	-2.8	-3.5	13.1	2.2			
							-0.2	7.1	8.8	15.8	4.0	0.9	0.5	1.3	0.3	2.1	9.7	7.8	1.9	4.1	0.9	2.7			
	6	4	6	6	6	6	6			-19.1	-24.0							-13.7	-12.7			11.8			
										10.0	16.8							9.4	9.6			0.8			
	4	6	4	6	4	6	4				-12.7														
											9.6										3.3				
	4	4	4	4	4	4	4				14.7														
											10.5										5.1				
	6	6	6	6	6	6	6			-14.6	-19.0								-12.7	-7.8			12.2		
										8.3	14.2										-9.1	6.9			0.9
	6	4	6	4	6	4	6			-17.5	-20.7									-12.4	-10.9			11.1	
										9.4	15.1										8.9	8.5			0.8
	4	6	4	6	4	6	4				-10.9														
											8.5										3.0				
	4	4	4	4	4	4	4				-12.7														
											9.5										4.6				
	6	6	6	6	6	6	6			-13.2	-19.4									-12.2	-8.1			11.0	
										7.4	14.4										8.1	6.8			0.7
	6	4	6	4	6	4	6			-16.0	-21.1									-11.9	-11.2			9.9	
										8.5	15.4										7.9	8.6			0.6
	4	6	4	6	4	6	4			3.0	-6.4	-6.2	-11.1	-2.7	-2.7	5.2	-0.9	1.8	5.6	-8.4	7.4	-1.1	-1.9	8.4	2.6
										0.2	6.3	3.9	8.6	2.0	0.7	0.3	0.8	0.2	1.3	5.5	1.7	0.8	0.9	0.6	1.6
	4	4	4	4	4	4	4				-12.9														
											9.6										4.6				
6	6	6	6	6	6	6			-12.4	-17.1										-11.6	-7.1			10.3	
									7.1	13.1										7.8	6.2			0.8	
4	4	4	4	4	4	4			-10.5	-18.7										-11.4	-9.9			9.3	
									8.0	14.0										7.7	7.8			0.7	
4	6	4	6	4	6	4				-9.8															
										7.8										-2.4					
4	4	4	4	4	4	4				-11.4															
										8.7										4.2					

Note: Shaded areas are normal stresses. Non-shaded areas are shear stresses.

Table 4.2 Shear and tensile stresses calculated for interior condition

Season of Placement	Time of Placement	Line of Analysis	Overlay Thickness (in.)	Slab Coeff.	Overlay Coeff.	Slab Modulus	Overlay Modulus	Winter								Summer												
								6 AM				6 PM				6 AM				6 PM								
								12 hrs		24 hrs		12 hrs		24 hrs		12 hrs		24 hrs		12 hrs		24 hrs						
								2	4	2	4	2	4	2	4	2	4	2	4	2	4	2	4					
6,000	6	6	6	6	6	6	6	3.6	0.1	20.7	28.7	7.2	6.7	-	-	-	-	14.9	15.3	3.1	3.8	-	-					
								0.0	0.1	11.5	21.4	5.3	1.5	-	-	-	-	11.0	12.0	2.4	4.8	-	-					
		4	6	6	6	6	6	6	6			23.1	30.3							14.8	18.0							
												12.5	22.3							11.0	13.6							
		4	6	6	6	6	6	6	6			11.3	17.6							10.4	7.5							
												6.8	13.4							7.5	6.5							
	4	6	6	6	6	6	6	6			13.8	19.3							10.1	10.3								
											7.6	14.3							7.4	8.0								
	4,000	6	6	6	6	6	6	6	20.3	27.1									14.5	14.7								
											11.3	20.7							10.8	11.8								
			4	6	6	6	6	6	6	6			22.6	28.5							14.3	17.2						
													12.2	21.5							10.7	13.2						
			4	6	6	6	6	6	6	6			11.3	16.7							9.9	7.4						
													6.7	13.0							7.3	6.4						
		4	6	6	6	6	6	6	6			13.5	18.1							9.7	9.9							
												7.5	13.7							7.2	7.8							
		6,000	6	6	6	6	6	6	6			16.7	24.5							12.3	12.9							
												9.8	19.2							9.3	10.7							
				4	6	6	6	6	6	6	6			18.9	25.9							12.1	15.4					
														10.8	20.1							9.2	12.1					
				4	6	6	6	6	6	6	6			9.1	15.0							8.3	6.2					
														5.6	12.0							6.3	5.7					
			4,000	6	6	6	6	6	6	6			11.2	16.4							8.3	8.8						
													6.5	12.8							6.2	7.1						
4					6	6	6	6	6	6	6			16.7	23.4							11.9	12.6					
														9.4	18.6							9.1	10.5					
4					6	6	6	6	6	6	6			18.6	24.7							11.8	14.8					
														10.6	19.4							9.1	11.8					
4,000				6	6	6	6	6	6	6			9.1	14.4							8.2	6.2						
													5.6	11.6							6.2	5.7						
					4	6	6	6	6	6	6	6			11.0	15.7							8.0	8.5				
															6.4	12.4							6.1	6.9				

Notes: Shaded areas indicate normal stresses.
 Non-shaded areas indicate shear stresses.

strains several days after the concrete member was cast. Few results are available that describe the development of strain at very early ages. Most published early-age results rely on the extrapolation of data collected from readings taken several days after placement. These data show that shrinkage strains in the first 48 hours generally range between 20 and 40 microstrain for normal weight aggregate. Laboratory and field studies at The University of Texas at Austin have shown that early strains were less than 25 microstrain at 48 hours. These data again rely on the extrapolation of results from readings taken at 3, 7, and 28 days. The strain at 24 hours, which corresponds to the conditions above, would cause a stress of 12 psi if fully restrained.

4.3 LONG-TERM EVALUATION OF BCO

The long-term evaluation of the pavement depends on traffic loading as well as on the environmental stresses induced on the pavement. Each of these factors is discussed below.

4.3.1 Traffic Loads

Van Metzinger (Ref 3) concluded that the crack spacing in the overlay and existing slab, existing pavement modulus and thickness, and overlay thickness influence the stress development in BCO. From the statistical analysis of field data, it was found that cracking can either be reflective or non-reflective. Before developing an analysis factorial from which equations for wheel load stresses can be developed, the effect of reflective and non-reflective cracking must be discussed.

Reflective Cracking

Figures 4.4 and 4.5 show reflective cracks and the corresponding distribution for a 3- and a 5-foot crack spacing. Figure 4.4 shows a load centered between the cracks while Figure 4.5 shows the loading on the cracks.

The stress distribution underneath each of these loads was calculated using an 8-inch existing pavement on a 6-inch cement-treated base with a 4-inch overlay. The stress at the crack can be evaluated and its importance is discussed later. The stress distribution between a 3- and a 5-foot crack spacing can be evaluated from these graphs, and the effect of non-reflective cracking can be compared to these graphs to establish an analysis factorial for evaluating wheel load stresses.

A slight increase in stress is found for the larger crack spacing versus the smaller crack spacing. The stress at the crack is also higher for the larger crack spacing. These stresses are compressive stresses that will eventually reduce the load transfer ability at the crack due to compression fatigue. Only the top 4 inches are in compression. The compression force is

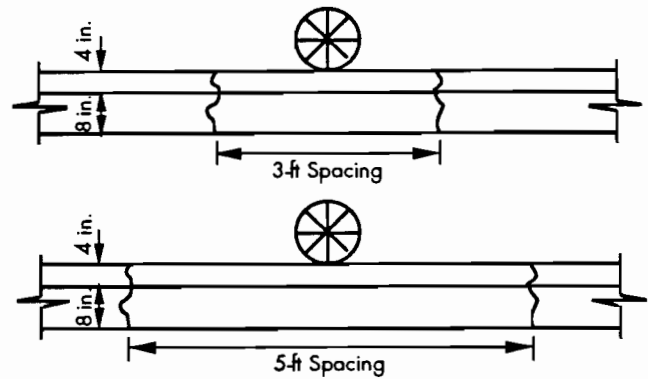


Figure 4.4a Wheel load position between cracks for typical crack spacings in BCO

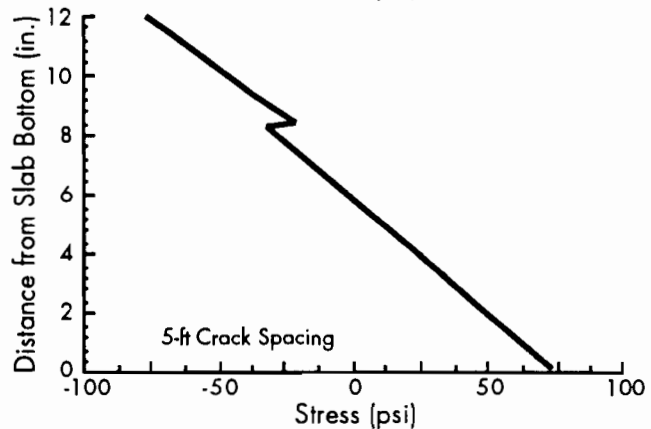
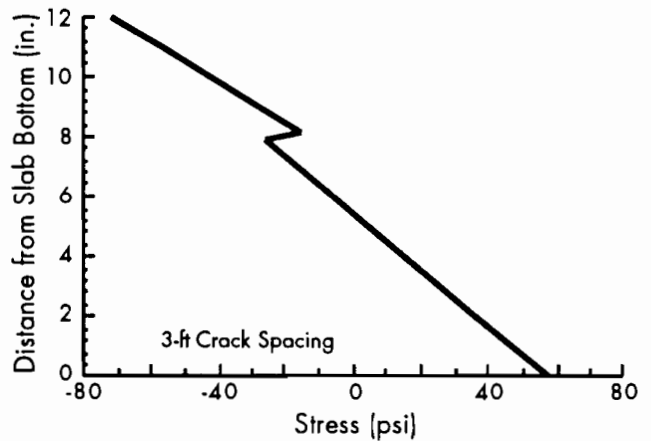


Figure 4.4b Stress distribution directly underneath load, load in center between cracks

Figure 4.4 Wheel load position and stress distribution for typical crack spacings in BCO with load between cracks

kept in equilibrium by the friction between layers and, slightly, by the reinforcing in the existing pavement. Lower in the slab, owing to the crack, the tensile stress should be zero. Small stresses shown in Figure 4.2 are due to the stress calculation procedure in the FEM program.

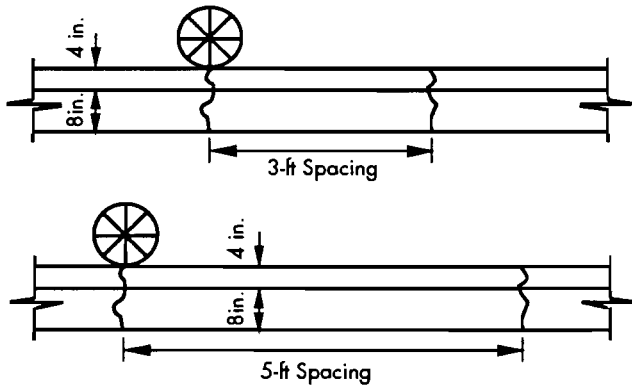


Figure 4.5a Wheel load position above crack for typical crack spacings in BCO

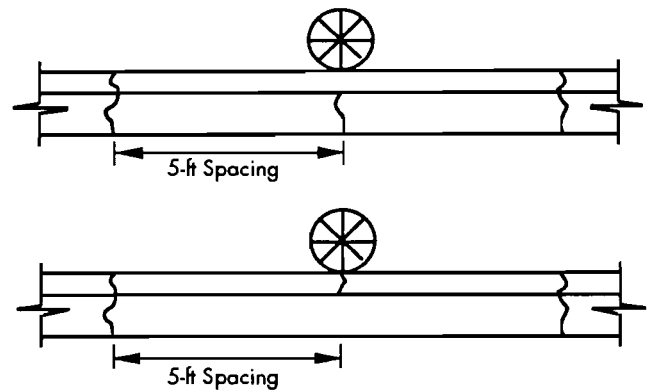


Figure 4.6 Scenarios for reflective cracking

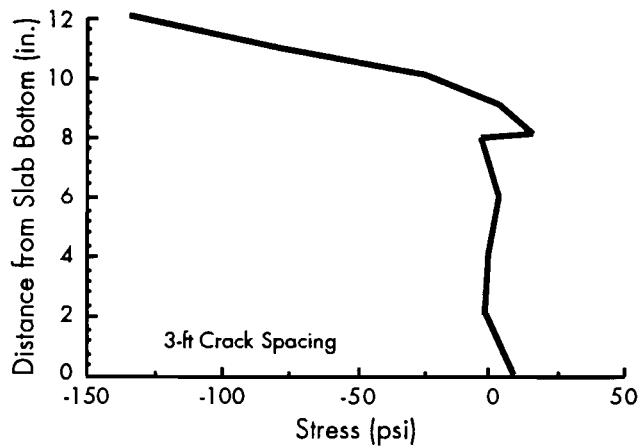


Figure 4.5b Stress distribution directly underneath load, load at crack

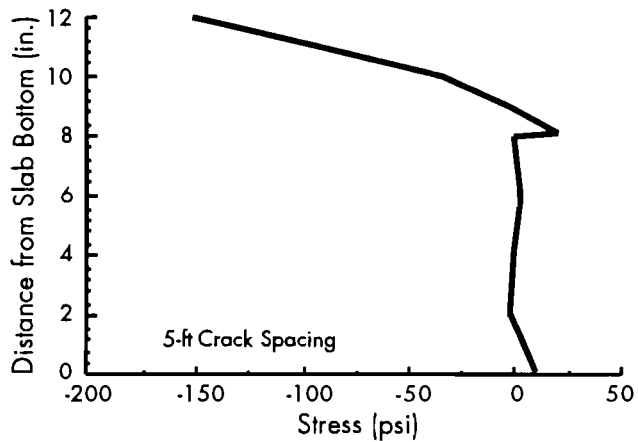


Figure 4.5 Wheel load position and stress distribution for typical crack spacings in BCO with load at cracks

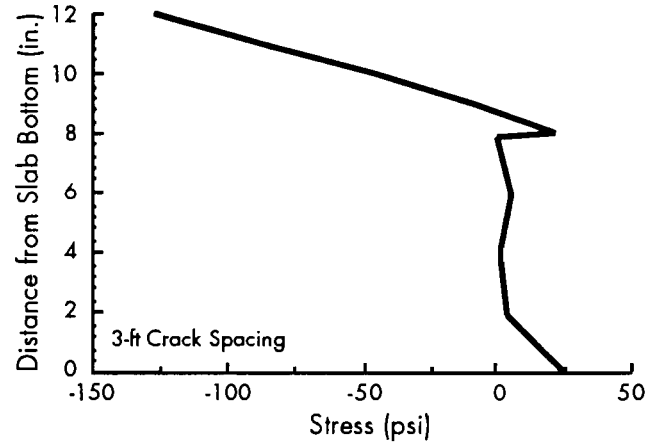


Figure 4.7a (Above) Overlay uncracked, existing pavement cracked

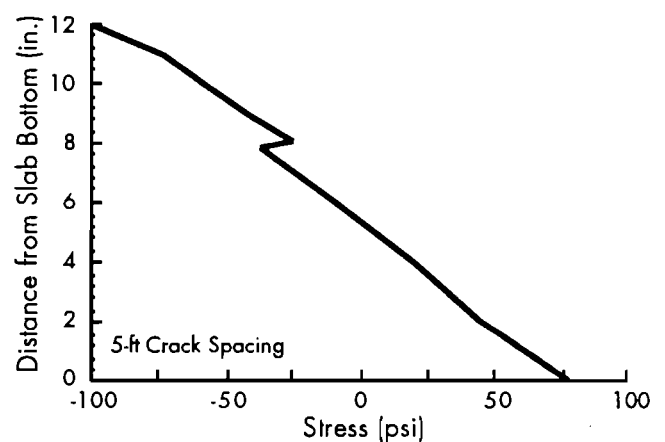


Figure 4.7b (Below) Overlay cracked, existing pavement uncracked

Figure 4.7 Non-reflective cracking scenarios

Non-Reflective Cracking

Figure 4.6 shows a typical layout of non-reflective cracks. For the purpose of this analysis a 5-foot crack spacing is assumed. Two scenarios exist. As shown in Figure 4.6, the existing pavement can be cracked with no cracking in the overlay or

the overlay can be cracked with no cracking in the existing pavement.

The stress distribution for the analysis of the two cases are shown in Figure 4.7. Figure 4.7a coincides with Figure 4.6a and Figure 4.7b coincides with Figure 4.6b. If these two figures are compared to the

figures for 5-foot crack spacing stress distributions (Figures 4.4 and 4.5), it can be seen that only minor differences exist in the magnitude of the stress and that approximately the same distribution exists. When a crack non-reflective crack exists in the overlay, a wheel load will put most of the crack in compression and all of the tension in the existing pavement, which explains why similar stresses are obtained. From this, it can be concluded that the maximum tensile stress is not influenced by cracking in the overlay and that the evaluation can be made at the center between cracks.

4.3.1.1 Wheel Load Stresses

The maximum stresses at crack spacings of 5 feet or greater are approximately equal (Ref 3). Therefore, only crack spacings of 5 feet or smaller are considered. Table 4.3 shows a layout of an analysis factorial to calculate maximum tensile stresses between cracks. The factorial is analyzed at three load levels. The three load levels selected are 9,000 pounds, 12,000 pounds, and 18,000 pounds.

Table 4.3 Analysis factorial for wheel loading

Crack Spacing Elastic Modulus: Exist Pvt Overlay Thickness Exist Pvt Thickness		Load Case 1					
		CS1			CS2		
		E1	E2	E3	E1	E2	E3
De1	Do1		X			X	
	Do2		X			X	
	Do3		X			X	
De2	Do1	X	X	X	X	X	X
	Do2	X	X	X	X	X	X
	Do3	X	X	X	X	X	X
De3	Do1		X			X	
	Do2		X			X	
	Do3		X			X	

A k-value was also included in the analysis and was calculated using the Eisenmann method (Ref 4). An equation was developed from the stress analysis for the maximum tensile stress at the bottom of the pavement.

Equation 4.1 was developed from the stress analysis by van Metzinger (Ref 3). It is very similar

to the Westergaard equation: if compared to the Westergaard equation, stress values will compare favorably, although some variation will exist. The variation is attributed to the use of a plane strain FEM program to analyze a three-dimensional problem.

$$\sigma = 0.288 * [P / (D_o + D_e)^2] * \{ \ln(CS) * \ln[((E * (D_o + D_e)^2) / 12 * k)^{0.25}] \} \quad (4.1)$$

where

- σ = maximum tensile stress at bottom of slab, psi;
- P = wheel load, pounds;
- D_o = overlay thickness, inches;
- D_e = existing pavement thickness, inches;
- CS = crack spacing in existing pavement, feet;
- E = modulus of elasticity of existing pavement, psi;
- k = modulus of subgrade reaction, pci.

As the crack spacing is reduced, the tensile stress perpendicular to the cracks is reduced. At 5 feet the stress is the same as the Westergaard stress, but below a crack spacing of 5 feet the stress is reduced. The spacing of longitudinal joints (cracks) formed by sawcuts on highways is typically 12 feet. This means that the stress in the transverse direction will be higher than in the longitudinal direction. The failure mechanism for overlays will, therefore, be the same as for other CRC pavements; i.e., a punchout will eventually form. This presumes that the interface remains intact throughout the life of the overlay. The fatigue factor at the interface is unknown. As the working crack loses its ability to provide load transfer, an uncracked overlay may crack or delaminate and small overlay punchouts may form. We can, therefore, conclude that Equation 4.1 can be used to evaluate stresses at small crack spacings.

The condition of the existing pavement at the time of overlay placement was also investigated. The basis of stress calculation is the stress at the bottom of the BCO above a crack. The lower the load transfer at the crack, the higher the stress in the overlay.

The stress equation developed by van Metzinger (Ref 3) is

$$\begin{aligned} \sigma_{over} = & 209.773 + (9000/P) \{ -0.017931 E_e \\ & - (424232/E_o) + 205.74(D_o/D_e \\ & - (D_o/D_e)^2) - 22.942(D_e/D_o) \} \quad (4.2) \end{aligned}$$

where

- σ_{over} = stress at the bottom of the overlay above the crack in an existing pavement, psi;
- P = wheel load, pounds;
- E_e = existing pavement modulus of elasticity, ksi;
- E_o = overlay modulus of elasticity, ksi;
- D_e = existing pavement thickness, inches; and
- D_o = overlay thickness, inches.

By using this equation and the previous equivalent stress equation, stresses can be calculated for examining the stress level at which the pavement will operate. It was mentioned before that reflective cracking cannot be assumed as the norm. Therefore, as discussed before, at the time the pavement is opened to traffic a cracking pattern already exists. If the existing pavement has a low remaining life, which can cause high tension stress in thicker pavements and shear stress in thin pavements, then cracks in the existing pavement will reflect through and a system with a high percentage of reflective cracking will be created. Such cracking will cause large areas to have very short crack spacings and can lead to punchouts in the system. Therefore, if the remaining life produces stress values in the BCO above the crack higher than those at the bottom of the slab between cracks, then an overlay will deteriorate faster than the existing pavement. Block cracking will form, which can lead to punchouts. Thus, the fatigue life of the overlay at a non-reflective crack should be the same, or greater, than that for the between-crack fatigue life of the existing pavement. This will ensure good performance and minimize premature failures.

4.3.1.2 Effect of Delaminated Areas

In Chapter 2 it was concluded that a significant increase in transverse cracking occurs in delaminated areas. The effects on a delaminated area are modeled by using the FEM program. Figure 4.8 shows a typical delaminated area with a wheel load passing over it.

A typical section from the test sections in Houston was analyzed. A 10°F differential was used on the overlay and a 9,000-pound load was placed on the crack. Figure 4.9 show the stress distribution at

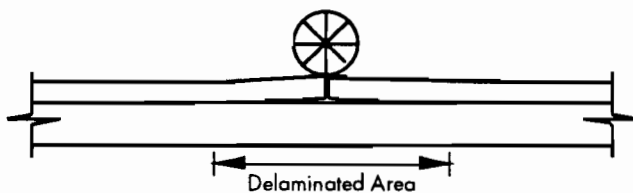


Figure 4.8 Delaminated area with wheel load passing over

the top of the overlay, for a distance of 18 inches from the crack. The pavement was modeled as delaminated for 18 inches on each side of the crack. When the temperature at the top of the overlay is lower than that at the bottom of the overlay, upward curling occurs. When the overlay curls, a cantilever is created, with the edge of the cantilever at the crack as shown in Figure 4.8.

It is evident from Figure 4.9 that a very high tensile stress exists at the top of the overlay owing to the cantilever action, because the temperature differential causes a small separation between the existing pavement and the overlay. As the wheel load passes, a high tensile stress is developed at the top of the overlay. The stress shown in Figure 4.9 is about one-third of the tensile flexural strength of the concrete. When this stress level is used in a pavement fatigue equation, the pavement will crack long before a crack is formed in the center of the 5-foot crack spacing section analyzed before. This explains the increase in transverse cracking in delaminated areas on the North Loop test sections in Houston discussed previously.

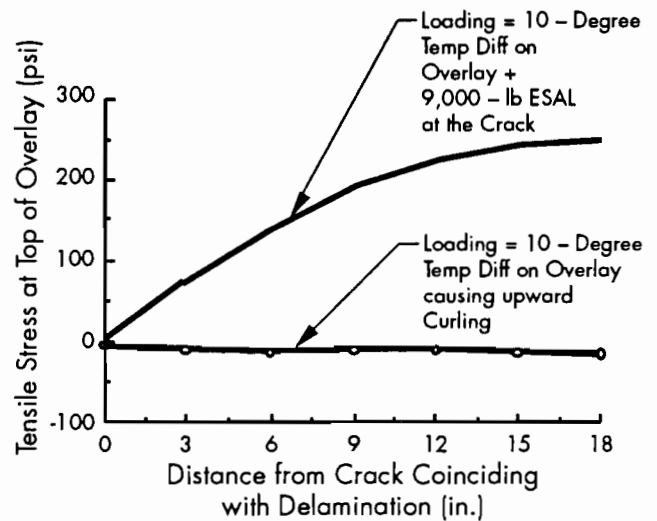


Figure 4.9 Tensile stress at top of overlay due to wheel loading

4.3.2 Environmental Stresses in BCO

The influence of environmental conditions on the performance of concrete pavements is well known. Concrete pavements are reinforced to control cracking caused by changing environmental conditions, such as temperature, shrinkage, and moisture movements. The influence of some of these environmental conditions on bonded overlays is discussed in the following paragraphs.

The environmental stresses when the existing pavement is cracked and the overlay is uncracked

and vice versa were analyzed. The results are shown in Figure 4.10 (page 24). It is apparent from Figure 4.10 that the stress at the crack is close to zero. The fact that some stress values are shown is due to the FEM program operation. The highest stress between the two cases is about the same. These stresses are not very high for an extreme case in Houston. The stress in this case is much lower than the tensile strength of the concrete. The important factor is, however, the shear stress at the interface, which is shown in Figure 4.11.

The shear stresses and tension stresses are much lower than the strength for shear and tension at the interface (Ref 3). The shear and tension due to wheel loading are also small, so we can conclude that these stresses will not influence the failure mechanism of the overlay. However, the fatigue mechanism of fatigue failure in shear or tension at the interface is unknown.

It is concluded from this section that the temperature stresses do not exceed the strength, and even with wheel loading included, the stresses are less than the strength. Because fatigue equations for the anticipated failure mechanism do not include

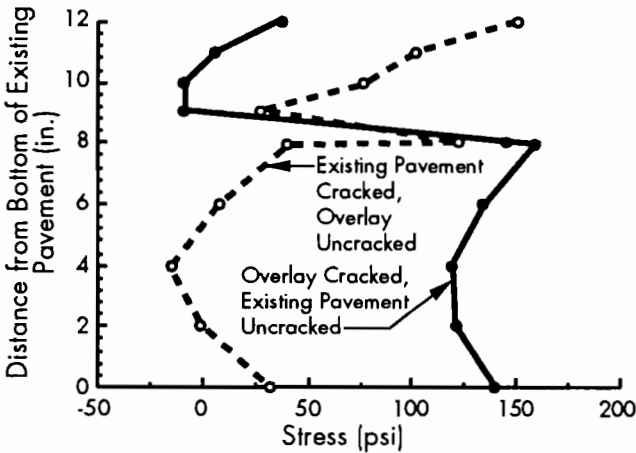


Figure 4.10 Normal stress through concrete section for existing pavement cracked, overlay uncracked, and existing pavement uncracked, overlay cracked

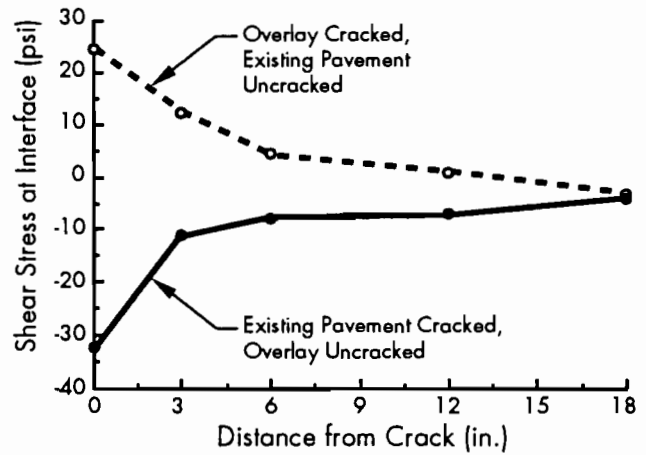


Figure 4.11 Shear stress at interface at cracks

temperature stresses, these were not used in the development of the design system proposed in this work.

4.4 CONCLUSIONS

Early-age stresses were found to be relatively low compared to the normal range of tensile stresses thought to cause failure in concrete. Furthermore, it was found that the stresses induced by early volume changes were small. However when these stresses are superimposed and compared to the available strength at the interface, it will be seen that the potential for delamination exists.

The wheel load stresses were analyzed and equations were developed for stress calculations in BCO (Equations 4.1 and 4.2). It was further found that a fully bonded concrete overlay will act as a newly constructed pavement, but that the remaining life of the existing pavement does influence the stress development of the pavement.

Finally, it is concluded that the shear and tension stresses are generally low at the interface and that no debonding should occur. It is also important to note that the stresses are much lower than 50 percent of the strength, which was a limit set by some researchers. The fatigue due to temperature loading occurs so slowly that the wheel load fatigue is probably more important.

CHAPTER 5. DEVELOPMENT OF AN EMPIRICAL-MECHANISTIC DESIGN METHOD FOR BCO

5.1 INTRODUCTION

The factors discussed and analyzed in the previous chapters are used in this chapter to form a design philosophy for BCO and to show the mechanisms of failure that can exist in BCO. This design philosophy is obtained from combining the results in the previous chapters into a design system that considers the long-term performance of bonded concrete overlays. The long-term performance model must be considered preliminary and will require modification as the existing overlays deteriorate and failure data become available.

The model is based on the punchout mechanism of concrete pavements, which is discussed later. Loading and thickness design are discussed in the following paragraphs. The conceptual mechanisms developed using the specific loading and overlay type and thickness are discussed later.

The environmental stresses are neglected because their influence on fatigue is considered minimal compared to wheel load stresses. These stresses are calculated for an 18-kip single axle. Equations were developed for stresses in bonded concrete overlay systems. These equations are used to calculate stresses and then to calculate the allowable number of applications. Miner's hypothesis can then be used to assure that the number of applications before failure is higher for the selected system than the number of applications needed to cause failure. However, because different failure criteria exist, the one that best suits the design system should be selected.

5.2 FAILURE MECHANISMS

The thickness design philosophy is based on the remaining life of the existing pavement and the expected future traffic. The stress equations discussed in Chapter 4 (Equations 4.1 and 4.2) are combined with equations developed elsewhere to assure that a selected failure criterion is met and that the performance of the overlaid pavement is as intended. The present serviceability index (PSI) is an index that portrays how well the road serves the user. Figure

5.1 shows the PSI versus time. Functional failure is when the road becomes unsafe or uncomfortable to use. The structural failure is a preselected level of distress (e.g., cracking or punchouts). The failure criterion selected for this work is 50 feet of cracking per 1,000 square feet of pavement. This relates to approximately 3 punchouts per mile per year.

Punchouts are the most important failure mechanism. From the field data analysis, three different structural failure mechanisms were identified. The first is a premature failure caused by debonding of the overlay. This failure mechanism cannot be used for design purposes because delamination is an early-age problem and with proper construction control it can be eliminated. With good bonding, the slab acts as a unit, and fatigue could be considered in the normal procedure. A model for delamination could be used to estimate the time before major repairs are needed, which would help in the distribution of funding at a project management level; however, the percentage delamination, for example, found on the North Loop in Houston is very small and does not justify the use of such a model. The second failure mechanism is punchouts in areas of non-reflective cracking and the third is punchouts in areas with reflection cracking.

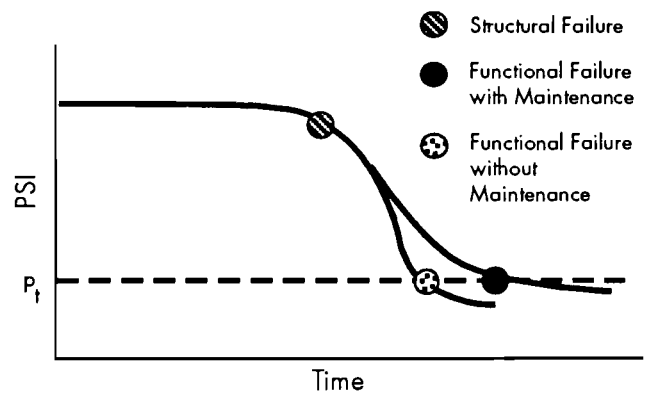


Figure 5.1 Present serviceability index versus time showing functional and structural failures

5.2.1 Punchouts in Delaminated Areas

Figures 5.2 through 5.5 show conceptually how the failure occurs. These sketches provide further insight into the failure mechanism of delaminated areas found on concrete pavements. Figure 5.2 shows an overlay with a delaminated area. In previous chapters it was shown that cracking in delaminated areas increases significantly compared to that in non-delaminated areas. The mechanism of failure was shown previously. The first step in the mechanism is therefore the formation of transverse cracks at the edge of the delaminated areas, as shown in Figure 5.3.

As the transverse cracking develops, the delaminated area forms an unbonded beam as wide as the delaminated area, which is kept intact only by the reinforcing steel. However, because it is an unbonded system, tensile stresses develop at the bottom of the overlay, as shown in Figure 5.4. This causes longitudinal cracks and eventually a punchout in the overlay, as shown in Figure 5.5.

The areas in Houston surveyed in 1990 still have not produced a significant increase in overlay punchouts, although the delaminated areas are nearing the end of the fifth year under traffic. The traffic loadings varied from 500,000 to 1,600,000 18-kip ESALs. The rate at which failure occurs once debonding has been found is slow, at least in the

Houston overlays. However, for non-overlaid CRC pavements, the rate of failure increases rapidly near the end of their lives and the same may be true for delaminated areas in overlays.

5.2.2 Non-Reflective Cracking Areas

The mechanism of structural failure in areas with non-reflective cracking is uncertain owing to the lack of data demonstrating failure. Depending on the state of the existing pavement, the existing crack may reflect through, and closely spaced cracks may develop in the overlay. The block of concrete between the transverse and longitudinal cracks is cracked on all four sides of the overlay, but on only three sides of the existing pavement. The longitudinal cracks can be either reflective cracks from the existing pavement structure or cracks due to shrinkage during the initial hardening period. The mechanism of failure can then be either that another crack forms in the existing pavement and a full punchout develops or that the section of overlay debonds. Debonding will occur only if high shear or tension forces are exhibited at the interface. This can happen if the existing cracks are wide enough for incompressibles to collect in the cracks. The mechanism is shown in Figure 5.6. This is very similar to the mechanism of failure for spalling of concrete pavements at cracks.

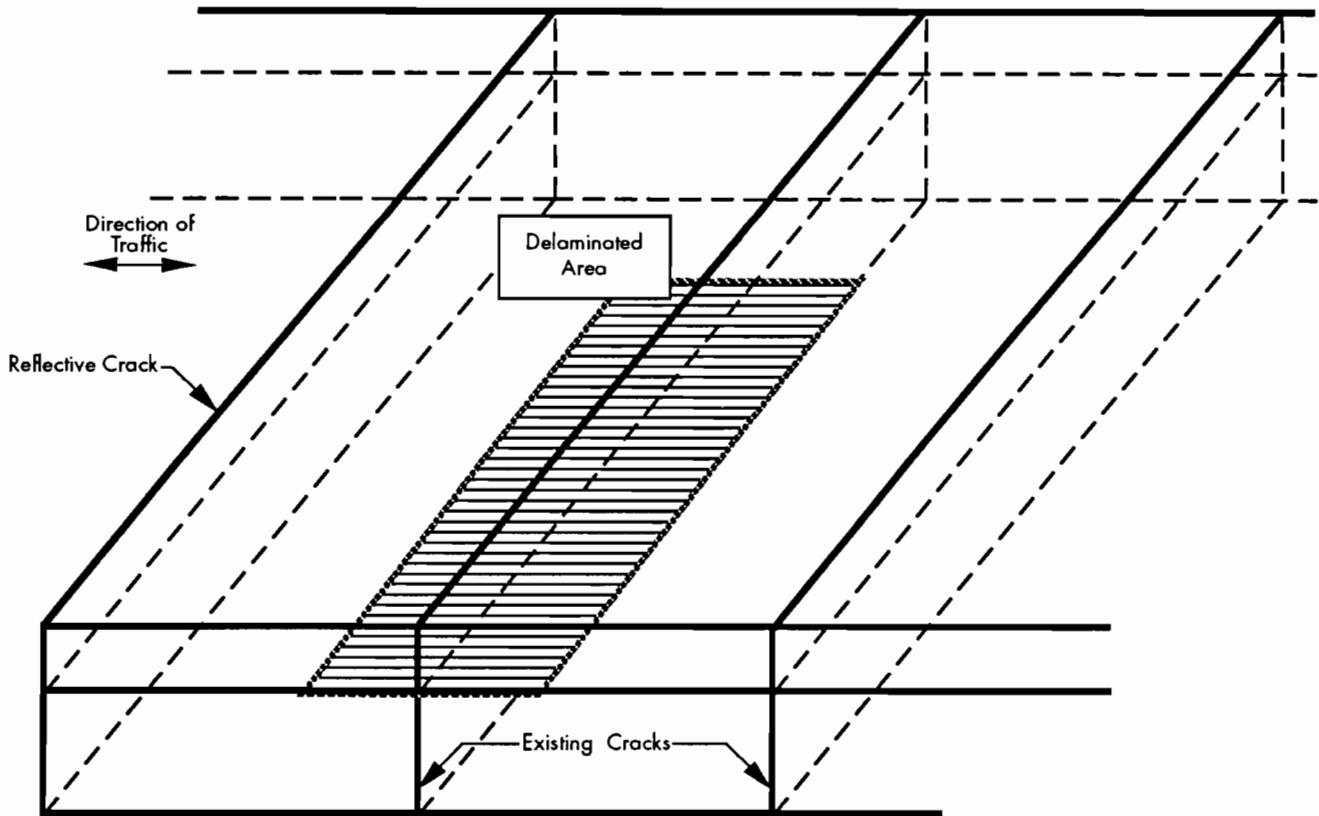


Figure 5.2 Delaminated area in BCO pavement

5.2.3 Reflective Cracking Areas

The mechanism proposed for areas where reflective cracking occurs is the same as that for newly constructed CRC pavements. As the crack spacing and load transfer at the crack are reduced, the transverse stresses become much higher than the longitudinal stresses, which increases the likelihood of longitudinal cracking. This is conceptually shown in Figure 5.7. The y-y stress is the transverse stress and the x-x stress is the longitudinal stress. Punchouts occur when longitudinal cracks are connected to transverse cracks. As Won (Ref 1) stated, the prediction of punchouts amounts to the prediction of the formation of longitudinal cracking. By modeling the longitudinal cracking, punchouts can therefore be predicted, which is an indication of the long-term, structural performance of the concrete pavement. Figure 5.8 shows a typical punchout in a concrete pavement.

The three structural failure types discussed can all occur. However, through good construction control, delamination can be minimized. For areas with non-reflective cracks, the failure mechanism is difficult to model because incompressibles infiltrate the pavement, especially where working cracks are wide. This produces high shear stresses when the pavement expands during the warm part of the day.

That leaves only the conventional punchout as a failure mechanism, and this is discussed further.

5.3 BCO CONSTRUCTION CRITERIA

In the first part of this chapter, structural failure and functional failure are discussed. From the PSI-time graph, shown in Figure 5.9, it can be reasoned that at some stage it is more economical to construct an unbonded overlay or to reconstruct, while at other times bonded concrete overlay construction is more practical. The point at which it is no longer feasible to construct a bonded overlay should be determined to ensure cost-effective performance of the rehabilitation. Field data on the pavement condition at which bonded overlays are no longer feasible do not exist. One possible criterion follows. As the existing pavement deteriorates, the effective modulus at a crack will decrease. If an overlay is placed over an existing pavement, the stresses at the crack and at the bottom of the overlay will depend on the stiffness of the existing pavement. As the load transfer is reduced at cracks, the transverse stress becomes the critical stress.

However, if the stress at the bottom of the overlay is high, a crack will form quickly and deteriorate to the state of the crack in the existing pavement. Furthermore, reflective cracks will also deteriorate to the state the existing crack was in before overlaying,

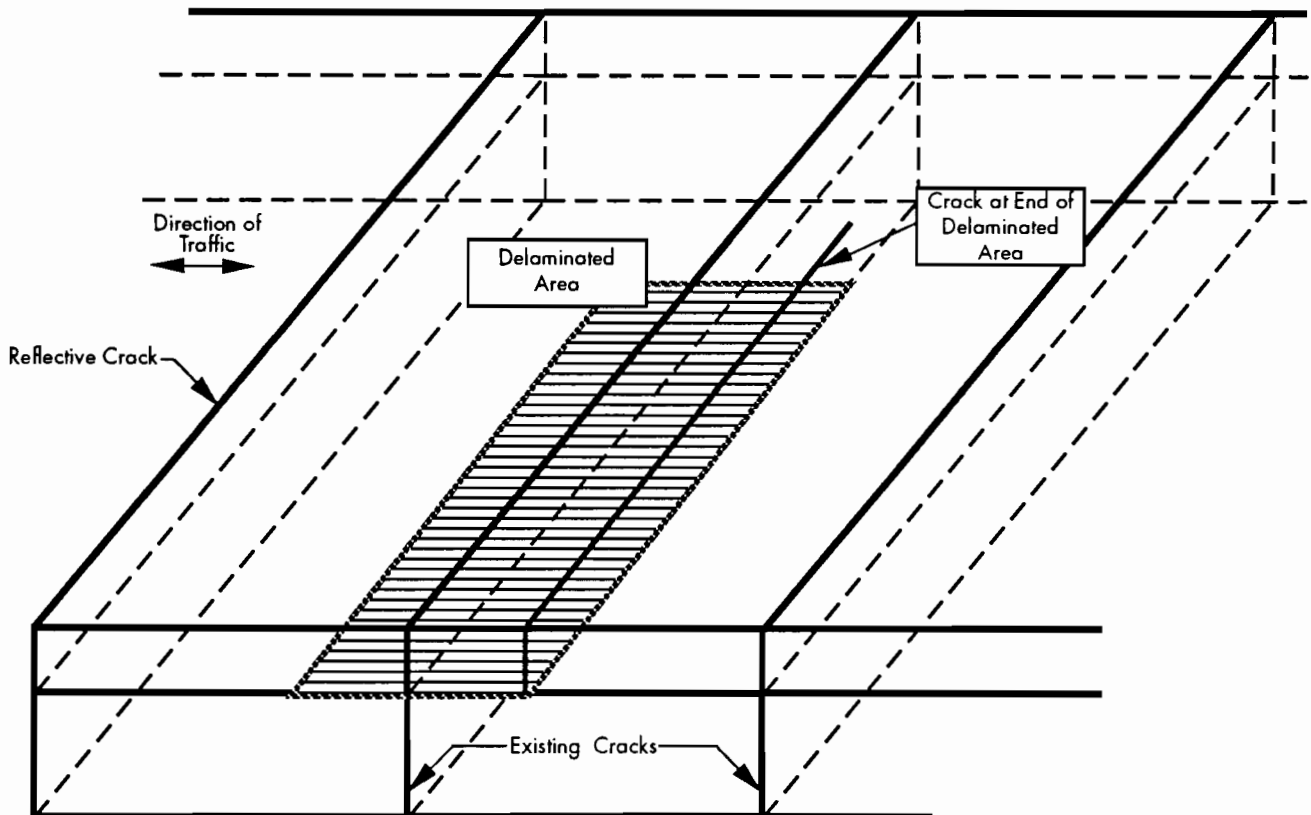


Figure 5.3 Transverse cracking in delaminated areas

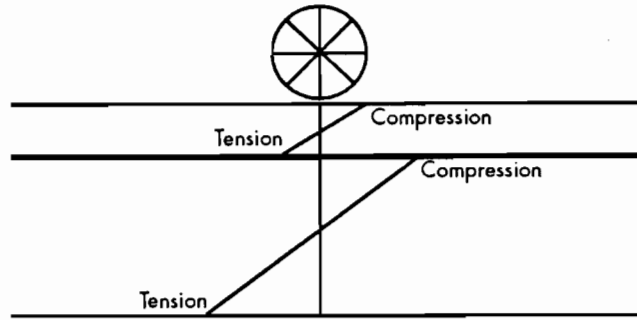


Figure 5.4 Conceptual stress distribution in delaminated overlays

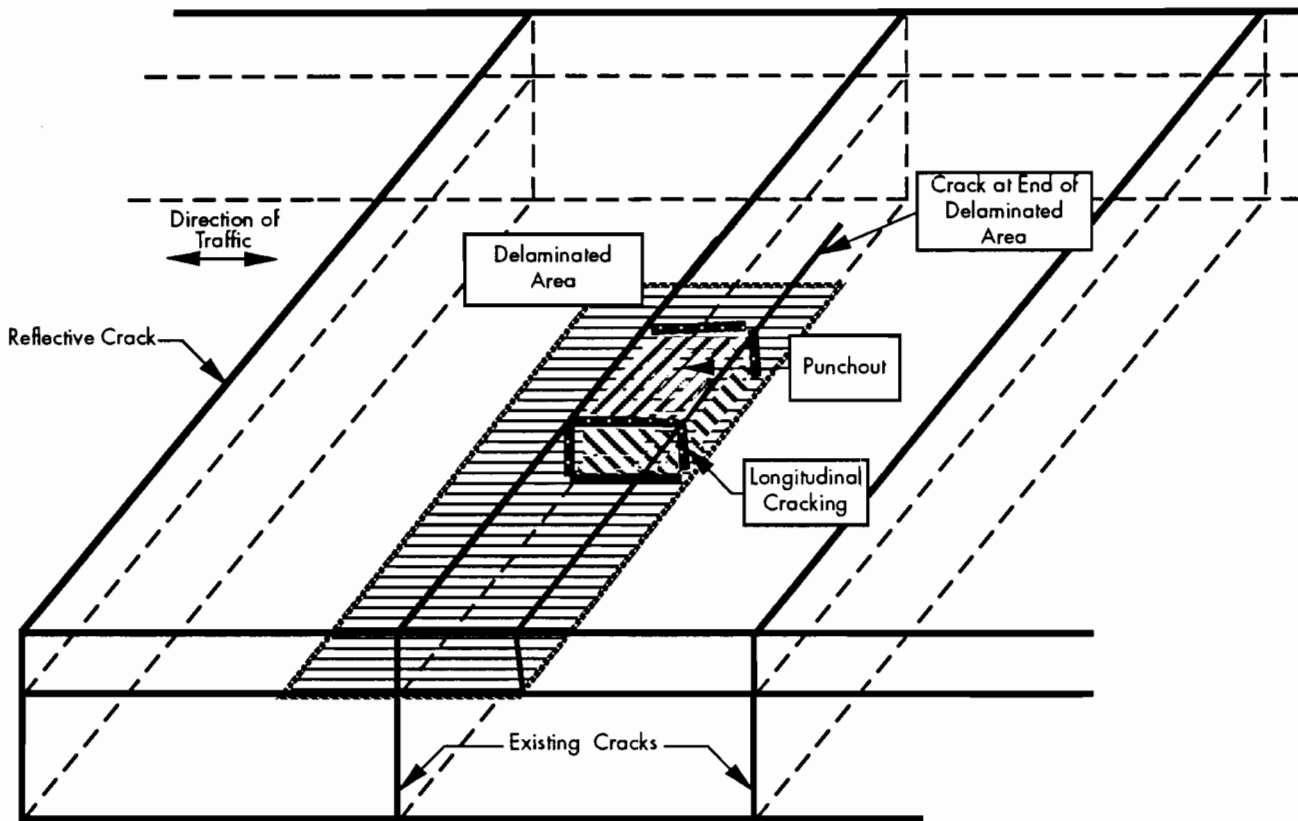


Figure 5.5 Longitudinal cracking development and punchout failure in delaminated areas

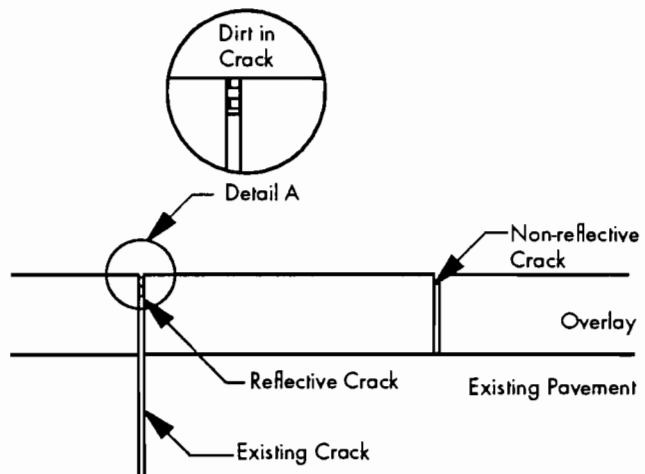


Figure 5.6 Mechanism for overlay punchout

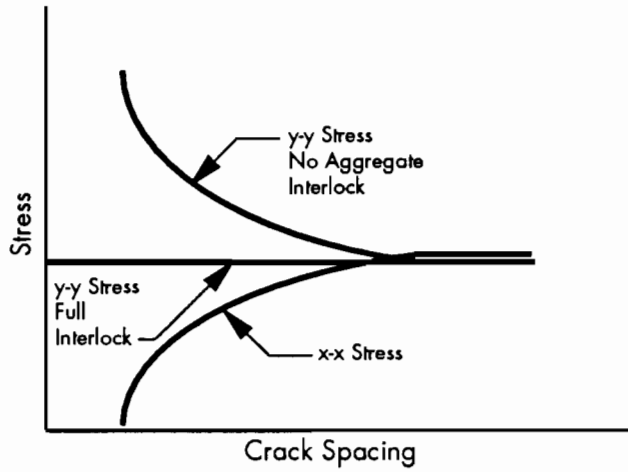


Figure 5.7 Conceptual layout of transverse and longitudinal stresses in PCC pavements

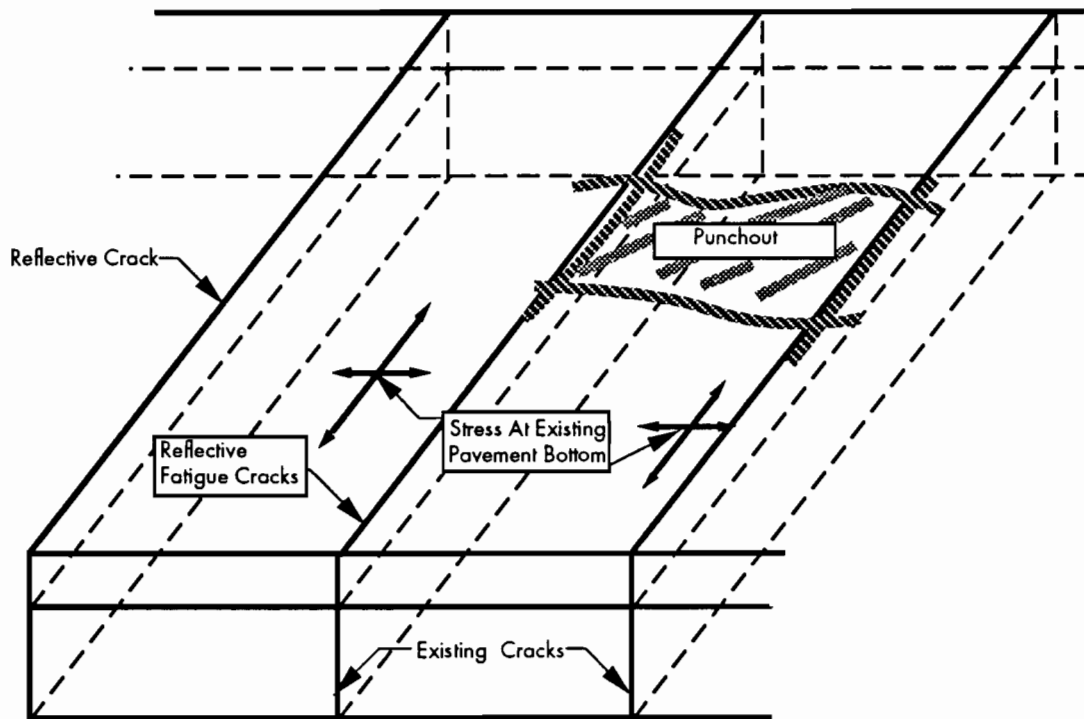


Figure 5.8 Typical punchout in PCC pavements

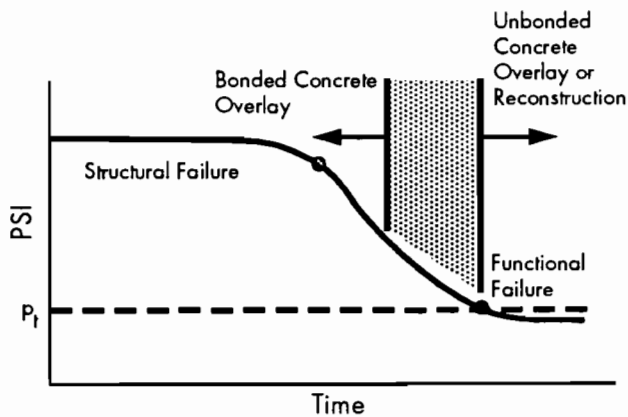


Figure 5.9 Time of type of overlay construction

as noted by Voigt et al (Ref 5). For the overlay method to be cost-effective, the stress at the bottom of the overlay must be less than the transverse stress at the bottom of the existing pavement.

This is so because the overlay will not fail before a longitudinal crack is formed. If the stress in the overlay is higher than the transverse stress, then the overlay will crack first, or a reflective crack will deteriorate quickly so that the transverse stress will increase. This increase in the transverse stress increases the probability of longitudinal cracking, which governs failure of the CRC pavements.

Van Metzinger (Ref 3) equated different deflections at the crack and at midspan for an existing pavement stiffness of 4,500 ksi at midspan. The deflection ratio at the crack versus at midspan was obtained and plotted against the stress ratio of maximum tensile stress in the overlay divided by full interlock transverse stress in the existing pavement. This is shown in Figures 5.10 and 5.11. In Figure 5.10 a BCO with a 4,500-ksi modulus of elasticity was evaluated, and a modulus of 6,000 ksi was evaluated in Figure 5.11.

From these two figures it can be concluded that, when a low modulus overlay such as a 4,500-ksi concrete is used, a BCO can be used as the overlay if the maximum crack deflection divided by the maximum between-crack deflection is less than 1.7. If a higher modulus concrete is used, a deflection ratio of 1.25 should be the limit. In addition to the deflection criteria, previous research has established that when the rate of punchouts/lane/mile/year reaches a value of three, the rate compounds rapidly. Thus, this value represents the outside limit for the feasibility of a BCO.

This is the first step in the design process. If a BCO is advisable, the next step is to design an

appropriate thickness for the anticipated design life traffic.

5.4 THICKNESS DESIGN

A design process for bonded overlays must be considered a two-step procedure. First, it must be determined whether or not the existing pavement is a candidate of a bonded overlay. Second, the thickness required to support the expected traffic is determined. The design system proposed in this work is diagrammatically shown in Figure 5.12 with the figures and equations that should be used in the calculation. It is a typical design procedure.

The thickness design depends on the remaining life of the existing pavement. By using a method such as the one described in the AASHTO Guide, a remaining life for the existing pavement can be calculated. Therefore, by selecting a thickness for overlay, calculating the stress decrease due to the overlay, and evaluating the pavement with some type of long-term performance model, an overlay thickness can be selected that produces adequate structural support for the expected level of traffic. The next section discusses a long-term performance model that can be used.

From the data and computer analysis done by van Metzinger (Ref 3), it was found that as the crack spacing is decreased the longitudinal stress between cracks is reduced. This finding corroborates the work of Won (Ref 1). With a crack spacing less than 6 feet, as is the case for most of the BCO constructed in Houston, the transverse stress is the controlling stress. When an overlay is placed on top of the existing pavement, it increases the thickness of the pavement but also restores load transfer at cracks. This is conceptually shown in Figures 5.13 through 5.15.

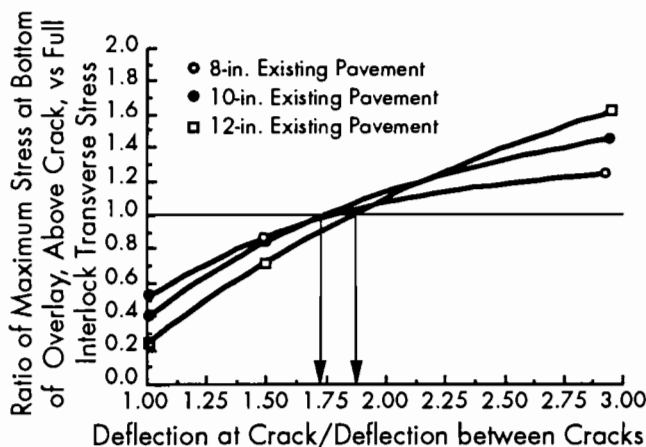


Figure 5.10 Stress ratio versus deflection ratio for overlay modulus of elasticity of 4,500 ksi

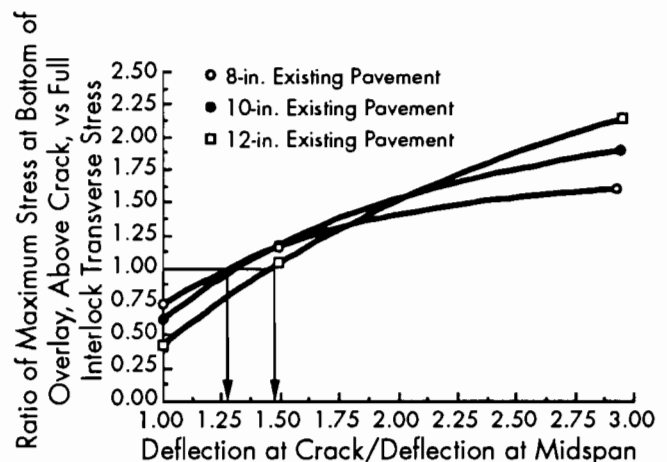


Figure 5.11 Stress ratio versus deflection ratio for overlay modulus of elasticity of 6,000 ksi

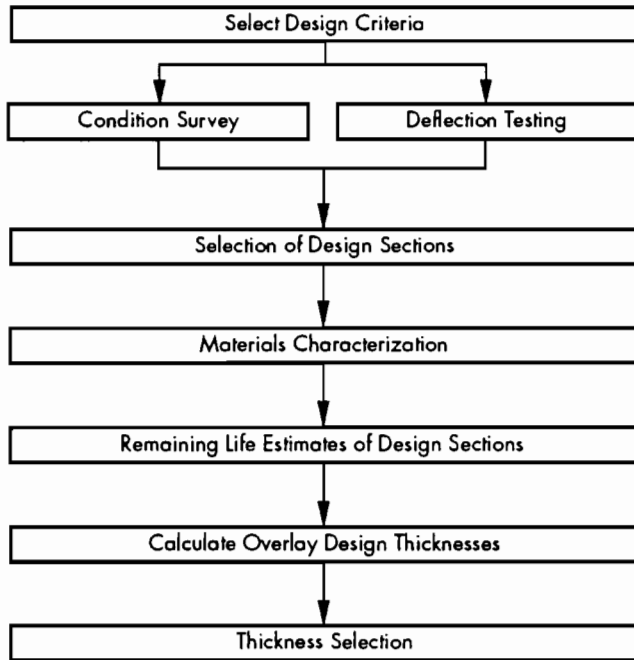


Figure 5.12 Diagrammatic layout of proposed design procedure

In Figure 5.13 it can be seen that, depending on the crack spacing, the transverse stress can be calculated. The x-x stress can be calculated using Equation 4.1 discussed before. The y-y stress depends on the quality of aggregate interlock. The lower the effectiveness of aggregate interlock, the lower the load transfer efficiency. As the load transfer efficiency (aggregate interlock) is reduced, the transverse stress is increased for a specific crack spacing. Because the stress at 6 feet is approximately the same for the y-y stress as for the x-x stress, as shown before, Equation 4.1, with a crack spacing of 6 feet, can be used to calculate the y-y stress for full aggregate interlock. The y-y stress for no aggregate interlock can be explained using the equation developed by Won:

$$\sigma = e^{9.8474 D - 1.8143 X - 0.4477} \quad (5.1)$$

where:

- σ = transverse wheel load stress for 9,000-lb load, psi;
- e = base of the natural log;
- D = pavement thickness, inches; and
- X = crack spacing, feet.

The stress changes, therefore, from full aggregate interlock during construction to a certain percentage thereof depending on the load transfer. Figure 5.14 shows a conceptual increase in transverse (y-y) stress due to a reduction in load transfer.

This curve depends on the type of load transfer installed, which will vary between aggregate interlock and a combination of aggregate interlock and

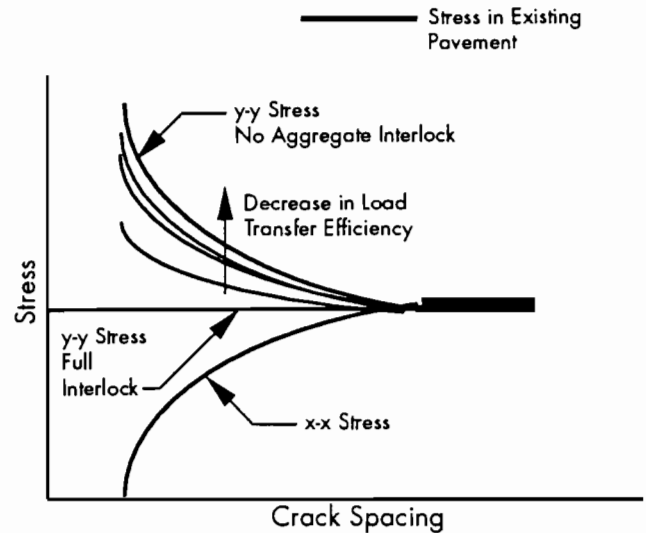


Figure 5.13 Stress in an existing pavement before overlay

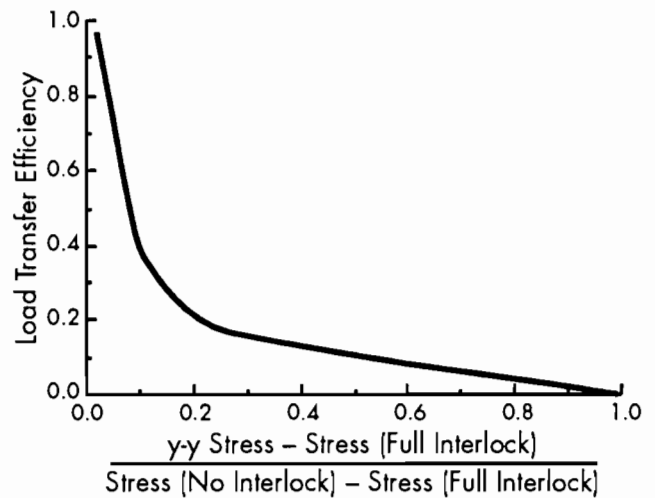


Figure 5.14 Load transfer versus increase in stress due to loss of load transfer

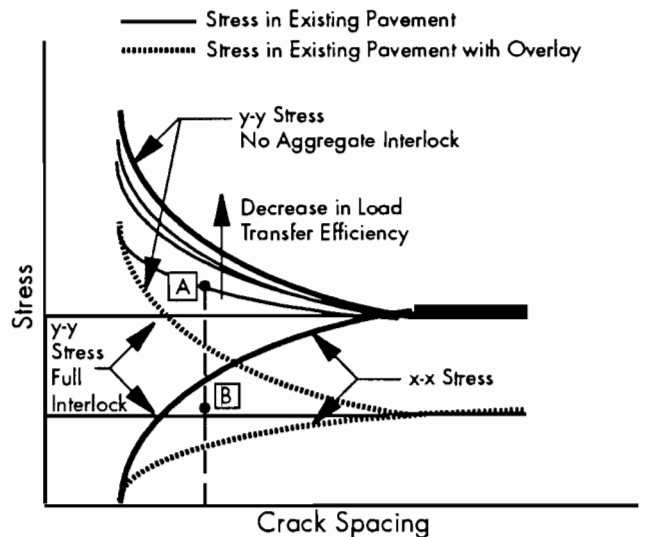


Figure 5.15 Stress distribution with overlay placed on existing pavement

reinforcing bars. However, a three-dimensional program that can model the effect is not available at this time. The form of the relationship in the reduction in load transfer is, however, close to what is seen in the field. Load transfer will stay intact for a long period, but when it starts to fail, the failure rate will increase significantly.

When an overlay is placed on the existing slab, the stress state changes from point A (Figure 5.15) to point B, which is a big reduction in stress and is due to the added thickness. Point B will initially be at the full aggregate interlock level and will deteriorate from there, as conceptually shown in Figure 5.11. In order to better quantify stresses, a relationship between reduction in load transfer and ESAL is needed, but that type of information is not available at this time. It has been concluded that, for a PCC concrete overlay of a 4,500-ksi modulus of elasticity, a BCO should not be constructed if the deflection at the crack divided by the deflection between cracks is more than 1.25. This is a load transfer efficiency of approximately 80 percent. We can then assume that during the life of the pavement, it will have, on the average, 80 percent load transfer efficiency.

It is therefore proposed that, until more data relating load transfer to time and longitudinal stress are obtained, the design stress for the overlay be calculated as

$$\sigma = \text{LTF}(\text{Stress}_{\text{no interlock}} - \text{Stress}_{\text{full interlock}}) + \text{Stress}_{\text{full interlock}} \quad (5.2)$$

The LTF is defined in this work as the load transfer factor. The load transfer factor is, therefore, dependent on the load transfer efficiency. For the above example, for a remaining life of 80 percent, the LTF is equal to 0.08 (from Figure 5.14). The governing stress can therefore be calculated for each thickness selected of the overlay to be placed on an existing pavement. The selection of a specific overlay thickness will depend on the thickness needed to satisfy the ESAL requirements obtained from a long-term performance model.

5.5 LONG-TERM PERFORMANCE PREDICTION MODEL

A design system proposed in the previous paragraphs depends greatly on the long-term performance model selected or developed. The method discussed above is based on a mechanistic approach derived from field observations that were recorded and then modeled. The long-term prediction model selected must incorporate the mechanistically developed part of the analysis and tie

it to the field performance. Because no long-term performance data are available for BCO, it is necessary to select existing equations that will best describe the model developed. Many fatigue curves are available. The development of longitudinal cracking is best described by Taute (Ref 6), who based his analysis on a cracking index of 50 feet per 1,000 square feet of pavement. He found that this failure condition corresponds approximately to a rate of defect of three defects (punchouts and patches) per mile per year. The model is

$$N = 46,000 (f/\sigma)^3 \quad (5.3)$$

where

$$\begin{aligned} N &= \text{Number of 18-kip ESAL,} \\ f &= \text{flexural strength of the concrete, psi,} \\ &\text{and} \\ \sigma &= \text{governing stress in the concrete, psi.} \end{aligned}$$

For each thickness selected, a method for predicting the governing stress was proposed in the previous section. The remaining life of the existing pavement is also known using the AASHTO guide method.

If traffic is used as basis for calculating remaining life, then the remaining life of the existing pavement, if we assume Miner's Hypotheses is valid, is

$$\text{Remaining Life} = 1 - (n_{\text{actual}}/N_{\text{predicted}}) \quad (5.4)$$

where

$$\begin{aligned} n_{\text{actual}} &= \text{actual number of ESAL during its} \\ &\text{life, and} \\ N_{\text{predicted}} &= \text{number of ESAL predicted} \\ &\text{(calculated) for the pavement.} \end{aligned}$$

The stress obtained from a specific thickness selected and used with Eq 5.2 should satisfy the following equation:

$$n_{\text{future}} = N_{\text{future predict}}(1 - (n_{\text{actual}}/N_{\text{predicted}})) \quad (5.5)$$

where

$$\begin{aligned} n_{\text{future}} &= \text{number of estimated ESAL for the} \\ &\text{design life of the overlay, and} \\ N_{\text{future predict}} &= \text{predicted (calculated) ESAL for a} \\ &\text{specific thickness.} \end{aligned}$$

The thickness that satisfies this equation will, therefore, be the selected design overlay thickness. Figure 5.16 shows the proposed design procedure diagrammatically, with the specific equations to be used for each section. Figure 5.16 is an expansion of the section "Calculate Overlay Design Thickness" in Figure 5.12.

Won (Ref 1) has shown a method of punchout prediction that can also be used for overlays and that could be used for budgeting for maintenance purposes.

5.6 CONCLUSIONS

A design method for BCO is proposed that is based on fatigue cracking of BCO. The knowledge gained from the statistical analysis of field data and

analysis using the FEM program was used to develop the design system.

However, the findings in this study should be verified using field data. It can also be concluded that BCO should not be placed if the deflections at the cracks are more than 1.25 to 1.7 times the between-crack deflections. Also, when the rate of punchouts/lane/mile/year reaches a value of three, the feasibility of a BCO is limited.

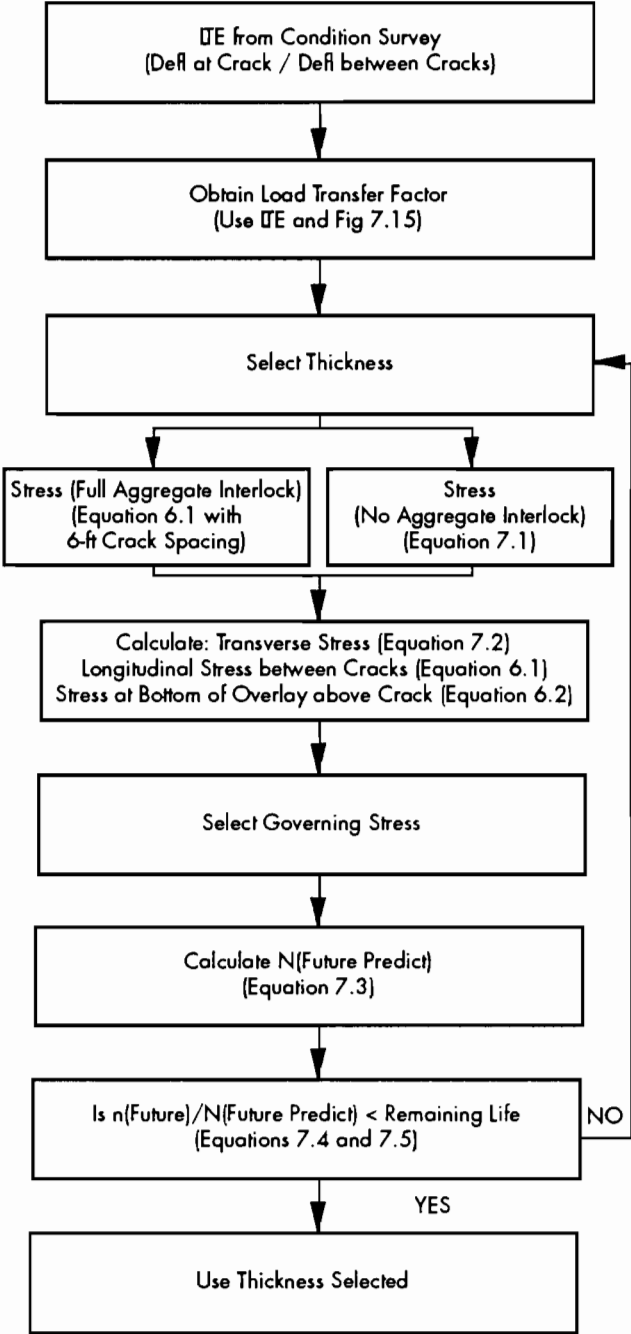


Figure 5.16 Diagrammatical layout of proposed design procedure

CHAPTER 6. CONSTRUCTION CONTROLS

The objective of this chapter is to provide guidelines that will reduce the risk of delamination at early ages. Even though the calculated interfacial stresses were considerably less than the estimated interfacial strength for all combinations investigated (Ref 2), delamination has occurred on several overlay projects throughout the country. Therefore, there must be combinations of environmental conditions and materials that result in debonding. These critical combinations can be avoided, and the probability of delamination reduced, through a proper design and careful control of the overlay construction.

The experience gained during the computer analysis and from construction will be combined to assure, to the extent possible, that early-age delamination will not occur. The calculated tensile and shear stresses are compared to the expected strength at the interface to allow for the selection of appropriate material combinations, construction procedures, and specifications that minimize the chance of delamination. The development of these guidelines is divided into three categories: (1) design, (2) specification, and (3) construction. While adherence to these guidelines will not guarantee the long-term success of the overlay, experience to date has shown that, if the overlay does not debond at early ages, then the rehabilitation will likely be a success. Therefore, the early-age performance, particularly with regard to the prevention of debonding, is paramount to the success of the overlay.

6.1 DESIGN

Many criteria are used to determine the most appropriate rehabilitation alternative for continuously reinforced concrete pavements. Among the criteria considered are the condition of the pavement, the user costs during construction, traffic handling procedures, expected traffic, and life-cycle costs of various rehabilitation options. The previous chapter provided guidelines for determining whether an existing overlay was a suitable candidate for rehabilitation using bonded overlay. Assuming that after consideration of these criteria a bonded overlay is deemed the most appropriate alternative, then every effort

must be made to ensure that the overlay will perform as intended. The long-term performance of the overlay depends on several factors, which were discussed in considerable detail previously. If these features are taken into account, then the success of the overlay at early ages is dependent on the two design parameters that have the greatest influence on the interface stress. These two parameters are the thickness of the overlay and the type and location of the reinforcement.

6.1.1 Thickness

The selection of the thickness of the overlay must include consideration of four criteria. First, the thickness must be sufficient to carry the expected traffic. Second, the impact of the thickness on various physical aspects of the facility must be recognized. Thickness may affect the cross-slope drainage or overhead clearances. These considerations may preclude the use of thicker overlays, particularly in some urban areas. Limitations on clearances, and the increased project costs associated with raising overhead structures, would favor the use of thinner overlays. These factors are case specific and therefore will not be included in further discussions. Third, the overlay thickness may be considered an indicator of the frequency of required maintenance and the time to the next major rehabilitation, i.e., the long-term performance of the overlay. It is commonly assumed that, within limits, a thicker overlay will last longer with less maintenance than will a thin overlay placed under similar circumstances. Thus, with other things equal, thicker overlays would be favored owing to the lower life cycle and user costs. Finally, the early-age influence of overlay thickness must be considered. Here the role of thickness in increasing or reducing the interfacial stress is considered. Only the early-age structural implications of overlay thickness will be considered.

The results from the FEM analysis of 2- and 4-inch bonded overlays show that, in some cases, the interfacial shear and tensile stresses were lower for the 2-inch overlays than for the 4-inch overlays (Ref 2). This would lead one to think that the 2-inch overlay would be less likely to delaminate than the

4-inch overlay. However, an important feature is not the calculated stress, but the ratio of the interface strength to the stress for a given combination of materials. The strength-to-stress ratios for the material combinations used on the North and South Loops were averaged separately for the 2- and 4-inch overlays. When this was done for all seasons and times of placement, it was found that there was no clear superiority between the two thicknesses. These data are shown in Table 6.1. Therefore, given that a shorter service life is expected from a 2-inch overlay, 4-inch overlays have an advantage.

Table 6.1 Strength-to-edge stress ratios for 2- and 4-inch-thick overlays similar to those placed on Loop IH-610 North and South, Houston, Texas

Material Combination	Stress	Overlay Thickness	
		2 in.	4 in.
North Loop	Shear	9	13
	Tensile	29	13
South Loop	Shear	20	21
	Tensile	33	24

Limited analyses were conducted on 6-inch overlays to determine the strength-to-stress ratios for thicker overlays. While there is a slight increase in the stress in the thicker overlay (about 5 percent), the difference in the strength-to-stress ratio is not significant. Overlays thicker than 4 inches are not normally used because of the additional loss of overhead clearance.

Field experience in the Houston, Texas area has shown that 2-, 3-, and 4-inch bonded overlays can be successfully placed on existing 8-inch CRC pavements under a variety of environmental conditions. Current design practice favors the placement of 4-inch overlays. This decision is predicated on the assumption that thicker overlays will last longer than thinner overlays and that overlays thicker than 4 inches cause an unnecessary reduction in overhead clearance. However, when overhead clearance is not a limiting factor, there is no reason why a 6-inch bonded overlay could not be used, based on early-age criteria.

6.1.2 Reinforcement

The FEM analysis of reinforcement in bonded overlays was severely limited by the implementation of the bar elements in the program. Further limiting the analysis was the restriction on the total number of elements to be used in a given run. When considered together, these restrictions prevented locating reinforcement at the actual level of the mesh in the

field. This limitation is not considered particularly damaging in the early-age analysis of overlay, because of the low bond stress transfer potential of concrete at early ages. Field experience must therefore be relied upon to develop guidelines for reinforcement.

Field experience has shown that overlays can be successfully placed using welded wire fabric, steel fibers, or no reinforcement. The current design practice in the Texas State Department of Highways and Public Transportation (SDHPT) favors the use of steel mesh reinforcement in the overlay at the same percentage used in the existing CRC pavement. Steel mesh reinforcement is used for two reasons. First, should any debonding occur, the mesh will limit the safety hazard due to loss of the overlay under traffic by keeping the area in place until repairs can be effected. Second, it is felt that the use of the same percentage of steel in the overlay as that used in the existing slab will result in the same crack spacing and width in the overlay as was found in the existing slab. While the first reason is most certainly sound and, in fact, has been shown to be of value in the field, the second reason requires some additional discussion.

The crack pattern in the existing CRC pavement developed as a result of the curing temperature, concrete strength, subbase friction, early-age environmental conditions, and years of traffic loading. Even if materials similar to those in the existing slab are used in the overlay, it is unlikely that a similar pattern will develop in the overlay as a result of the use of the same amount of steel. The environmental conditions, physical dimensions, and the restraint of the underlying layers are completely different. It is possible, however, that if the cracks in the existing slab reflect through the overlay, the reinforcement will control the crack width in a manner similar to that of the existing slab steel. Surveys of in-place overlays in Texas have shown, however, that many non-reflective cracks form (Ref 3).

The presence of non-reflective cracking further compounds the problem of determining the influence of the reinforcement. Texas SDHPT designs currently allow the mesh to be placed directly on the existing CRC. Examination of Figure 6.1 (page 36) shows the influence of reinforcement on reflective and non-reflective cracks. The usefulness of the steel in limiting the crack width in reflective cracks is clear. If there is full coverage of the steel, two layers work together to limit the crack width. However, because of the location of the steel, little crack-width control can be gained from the steel in the case of the non-reflective crack. Here, the steel is located at the bottom of the layer, in what is a compressive stress zone. Therefore, if the steel continues to be placed directly on the existing slab, its main function

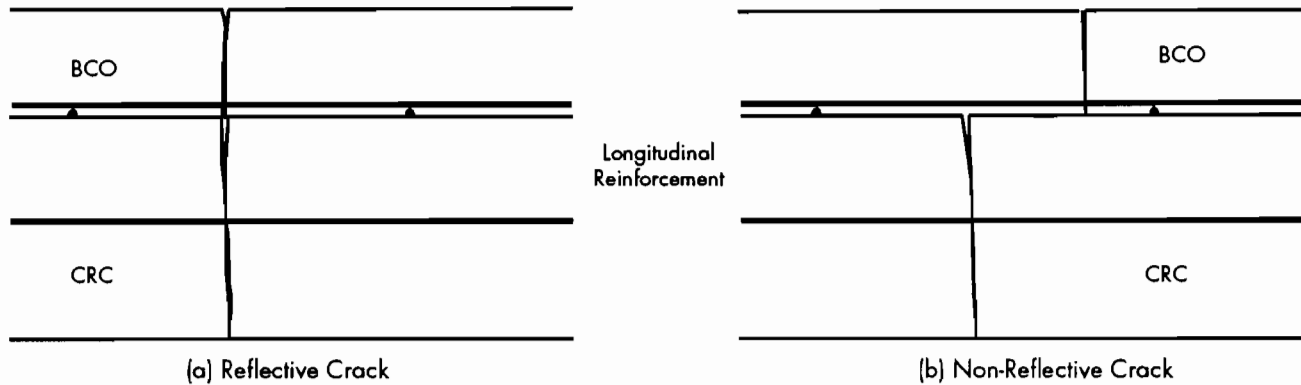


Figure 6.1 Schematics of the influence of steel on reflective and non-reflective crack-width control

will remain one of delamination-loss control. It may be possible to prevent the loss of any debonded areas under traffic with a lower percentage steel than that normally required to control crack width and spacing.

The impact of the layer of steel mesh at or near the interface on the strength of the bond between the two layers is not well understood. Logically, the introduction of a layer of steel mesh at the interface would adversely affect the strength. Only limited test results are available, but, when pull-out tests were conducted in one study (Ref 2), no significant difference in shear strength could be found when the reinforcing mesh was placed on the existing slab or at mid-depth in the overlay.

Although the vast majority of the overlays placed in Texas have been placed using steel mesh reinforcement, experimental sections have been constructed using steel fibers and using no reinforcement. A 2-inch bonded overlay without any reinforcement in Houston has been in service for seven years without any performance problems. The use of steel fiber reinforcement has been tested in three separate test sections placed over the course of six years. The test sections were placed under a variety of conditions. All are performing well, with little or no delamination.

6.2 SPECIFICATION

The specification and construction of bonded overlays are very important to the early-age success of the overlays. Because successful overlays have been placed using a variety of thicknesses and materials and several different types of reinforcement, it is likely that the specification of the overlay and the control of construction are paramount to the success of the overlays. There is no one item that is most important to the successful construction of bonded overlays and, therefore, the discussion that follows covers the construction of a bonded overlay from the selection of materials to the curing of the overlay.

6.2.1 Materials

The first step in construction is to select the materials for use in the overlay. The FEM analyses discussed previously showed that the use of aggregates for the overlay concrete that produce moduli and thermal coefficients lower than those found in the existing slab result in lower interfacial stresses regardless of the time or season of placement. This concept is expanded in Ref 2 through regression analysis, which shows that the interfacial stresses can be predicted for a given environment with a high degree of accuracy for a combination of overlay and existing slab material properties. This is important because the aggregate type has the major influence on the thermal coefficient and modulus of the concrete. A reduction in the elastic modulus of the aggregate normally results in a reduction of the concrete modulus and the thermal coefficient. This may not be the case with certain types of manufactured aggregates; however, within the limits of the regression analysis, these special cases can be accommodated.

Other materials of interest to the early-age development of stress in bonded overlays are the cement and admixtures used in concrete. In the past, Type I cement has been used successfully and, given the magnitude of the stresses developed at the interface, there does not appear to be a need to use high-early-strength cements. Petrographic analyses of cores taken from delaminated areas on Loop IH 610 North showed the early formation of the products commonly associated with alkali-aggregate reactions (Ref 3). The cause of these formations is not known, but the importance of maintaining the normal specification limit on alkali content should be emphasized.

The use of admixtures of various types is common in concrete pavement construction today. Retarders are used to allow adequate time for transportation and finishing the low slump concretes commonly used with slip form pavers. The

influence of these retarders, and other admixtures, on the rate of gain of interface strength is not known. It can be reasoned however, that, if the rate of strength gain in the concrete is substantially reduced, then the rate of interface strength gain will also be reduced. These lower strengths make debonding more likely for a given set of environmental conditions.

6.2.2 Surface Preparation

The next step in the specification of bonded overlays is to assure that the existing slab is adequately prepared to receive the overlay. Adequate preparation must include a thorough cleaning of the surface. Bonded overlays have been placed successfully on surfaces prepared using shot blasting, sand blasting, or coldmilling. The texture is much more angular after milling, compared to the rounded aggregate surfaces exposed after shot or sand blasting (see Figure 6.2). From the standpoint of mechanical interlock, the milled surface would be more appealing. However, milling relies on a fracturing of the surface, which may cause microfractures in the remaining material. The importance of this feature is not known, but it may account for the similar interface shear strengths found in milled and blasted surfaces (Ref 2). Therefore, based on strength alone, there is no reason to specify the method of surface preparation.

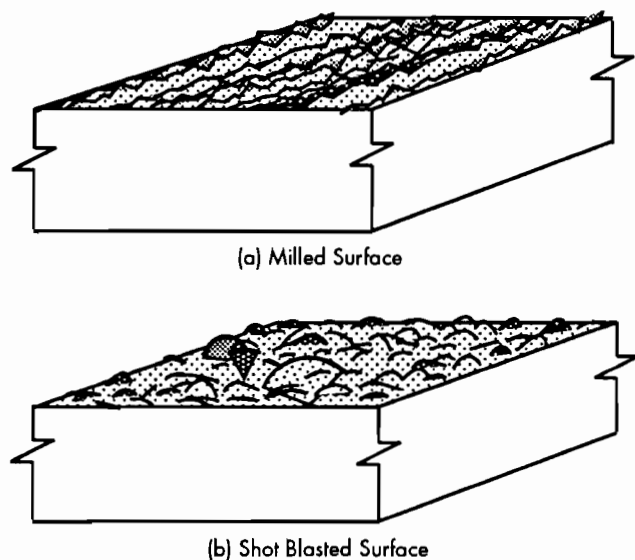


Figure 6.2 Schematics of milled and shot blast surfaces with equal texture measurements

Consideration should be given to the cost, rate of production, and environmental desirability of the various alternatives. Cost figures from the Houston area overlay projects indicate that the cost of shot

blasting is about one-half the cost of milling. These costs and the rate of production are controlled to some extent by the specification of the depth of removal or required texture. Shot blasting results in less environmental impact from the dust through the shot and dust recovery system included in the newer, self-contained, equipment. These factors will change from project to project, but the shot blast technique appears to be the most desirable.

If the method of surface preparation need not be specified to insure adequate bond strength, then the surface preparation must be specified in terms of the depth of surface removal or some standardized texture test method, such as the Texas Sand Patch Test, or a combination of the two. Both methods have advantages and disadvantages. Texture test methods have been standardized and therefore have some known repeatability and error. However, they have the disadvantage that tests can produce precisely the same value of texture for two completely different surface preparation techniques that have markedly different surface characteristics. These tests do not characterize the surface angularity or contour; only the average depth of the surface is determined. Laboratory and field testing have shown that adequate strengths can be obtained using either blasting or milling, and therefore this disadvantage is not significant.

The advantage of the specification of a particular depth of removal is that it assures that all surface contaminants are removed and that, if significant carbonation has occurred, this material will be removed. Also, in areas where salts are used to control ice, the specification of a depth of removal can insure that the highly sulfate-contaminated material is removed. When cold milling is used, determination of the thickness to be removed is relatively easy. However, the depth of removal is sometimes difficult to determine when shot or sand blasting is used and must depend on the experience of the inspector.

In summary, the specification of a surface preparation method is not necessary to assure bond strength. However, to insure that all contaminants are removed from the existing slab, a depth of removal should be specified. The removal of 0.25 inch of material is suggested, but a greater depth may be necessary in areas where sulfate contamination is common. The texture should be checked using the Sand Patch Test or an equivalent. Until other information is available, an average texture depth of 0.08 inch is suggested.

There are other controls which will be used in the construction of the overlay. These features will be included in the project specifications, but they will be discussed in conjunction with the construction of the overlay.

6.3 CONSTRUCTION

The control of the construction of the overlay is important if the probability of delamination is to be reduced. Beyond the normal construction controls that are used for any concrete paving job, certain controls are required that are specific to bonded overlay placement. These construction controls fall into three categories. First, there is a need for environmental controls that provide limits on the time and season of placement so that interfacial stresses can be minimized. Second, limitations on the bonding agent used and on the condition of the interface at the time the overlay concrete is placed are necessary. Finally, special precautions are necessary to insure adequate curing of the overlay.

6.3.1 Environmental Controls

The environmental conditions during and immediately after placement of the overlay play a very important role in the development of the interfacial stresses. It has already been shown that for a given combination of materials in the overlay and existing slab, the interfacial shear stress may be increased more than 500 percent, simply by placing the overlay in the early morning instead of the late afternoon. It is therefore prudent to include certain environmental controls during construction.

The analyses indicate that, even under the extreme conditions of time and season of placement, debonding will not occur. Initially, this would tend to indicate that environmental controls are not necessary to the success of overlays. However, the interface strengths used at the analysis times of 12 and 24 hours were based on a 7-day interface strength value of 200 psi. The results of laboratory testing of many different bonded overlay types constructed using a variety of surface preparation techniques and bonding agents show that in all cases the mean interface shear strength was in excess of 200 psi (Ref 2). Theoretically, there should be no debonding.

There is delamination, however, and an examination of the standard deviations of the means of laboratory data (Ref 2) indicates one possible reason for the occurrence of debonding. The one-tailed confidence intervals for α -levels of 1, 5, and 10 percent are shown for the shear strengths in Table 6.2. It can be clearly seen that, with the large standard deviation associated with the shear strength, a large percentage of the total population of any given type of BCO will fall below the suggested limit of 200 psi. Although it cannot be said with certainty, it is likely that the failures that have occurred on the North Loop came about as the result of low strengths combined with severe environmental conditions. This concept can

best be illustrated by consideration of the example discussed below.

Assume that a 4-inch overlay was placed on the North Loop under environmental conditions that produced a shear stress at the interface 24 hours after placement of 25 psi. This stress would develop in an overlay placed during a winter morning. If the interface shear strength throughout the placement is 200 psi at 7 days, then the estimated strength of 85 psi at 24 hours is adequate and no delamination will occur. However, as with other physical quantities, the interface strength has variability. In fact, in the case of the interface strength that variability is quite high.

For example, the average shear strength of 25 cores taken from the North Loop overlay project six months after placement was 387 psi. The standard deviation was 155 psi. Assuming the 7-day strength is 75 percent of the 6-month strength, then the strength at 7 days was 290 psi. From Ref 2, the 24-hour strength is one-third of the 7-day strength, or in this case 96 psi. If the magnitude of the coefficient of variation at 24 hours is assumed to be equal to the magnitude of the coefficient at six months, then the standard deviation at 24 hours is 38 psi. Now assuming that the interface strength is normally distributed, the α -level associated with the expected stress of 25 psi is 3 percent. Thus, about 3 percent of the overlay placed under these conditions would have an interface strength less than the stress, and debonding would result. The computed value is reasonable when compared with the extent of delamination on the North Loop. The percentage on Loop IH 610 North was approximately 1.1. The overlay on the North Loop was placed under a variety of conditions, which could account for the differences.

Table 6.2 One-tailed confidence limits for 7-day laboratory shear strength

Surface Preparation	Bonding Agent	Mean Shear Strength (psi)	Confidence Interval		
			90%	95%	99%
Light Shot Blast	Latex	638	346	263	108
	Epoxy	661	338	264	75
	PCC	471	126	28	-
	None-Dry	488	226	152	13
	None-Wet	430	183	112	-
Heavy Shot Blast	Latex	605	473	436	365
	Epoxy	608	281	188	15
	PCC	746	385	282	90
	None-Dry	695	560	522	450
	None-Wet	527	327	270	164
Cold Milling	Latex	679	459	396	279
	Epoxy	654	300	200	12
	PCC	530	239	157	2
	None-Dry	460	146	57	-
	None-Wet	476	258	196	80

The occurrence of debonding depends on the variability of interfacial strength even though the average strength is well above the calculated stress. This would naturally lead to the desire to increase the interface strength through the use of different surface preparation techniques or bonding agents. However, research conducted at The University of Texas at Austin (Ref 2) has shown that there are no statistical differences among the various surface preparation methods or bonding agents commonly used today (with the exception of the latex-modified grout that performed unsatisfactorily). Therefore, if the average interface strength cannot be increased, then the variability of the strength must be reduced or the induced stress must be lowered.

The means by which the variability of the strength can be reduced are not known. Research conducted at The University of Texas at Austin (Ref 2) investigated modifying the rate of application of the bonding agent and the time from the application of the agent to the placement of the overlay. These factors did not have a significant effect on the average strength or the variability of that strength. Until information can be found on ways of reducing the variability of the strength, other means of decreasing the occurrence of delamination must be found. These other measures will rely on reducing the induced stresses.

Environmental controls on the time of construction of bonded overlays provide a means of reducing the chance of debonding. Limits must be placed on the time of placement of the overlay, which will insure that stresses will remain below the expected strengths. The technique for implementation of these controls relies on an expected 7-day shear strength for the project, as determined by the direct shear test method described above. An acceptable level of debonding is selected, say one-half of one percent, and the maximum allowable interface shear stress is determined. The allowable shear stress is then compared to the stress calculated by the FEM program for the materials in the existing slab and for those selected for use in the overlay. By comparing the allowable stress for certain key environmental conditions, those seasons and times of placement that would cause failure are identified and can be avoided. Details of the method are described below.

The first step is to select a reasonable range of interface strengths. Seven-day interface shear strengths from 100 to 1,000 psi were chosen. Then, using the relationship between the 7-day strength and 24-hour strength shown in Ref 2, Figure 6.3 was developed. This figure shows the maximum allowable interfacial shear stress for the 24-hour time of analysis. Levels of reliability between 90 and 99.5 percent are shown. It should be noted that levels of reliability greater than 99.5 percent are not possible

because of the high variability of the strengths. The allowable shear strength and the associated tensile strength would then be compared to the expected stress, resulting from a given environmental condition to determine if an overlay should be placed. This procedure is described below. The equation relating 7-day shear strength and the maximum allowable shear stress is shown below.

$$\tau_{\text{allow.}} = x (S_{7\text{-day}} - \sigma Z_{1-\alpha})$$

where

- $\tau_{\text{allow.}}$ = allowable shear stress,
- $S_{7\text{-day}}$ = 7-day shear strength,
- σ = standard deviation of the shear strength,
- $Z_{1-\alpha}$ = Z-score associated with the desired reliability, and
- x = 0.256 for 12-hour analyses,
0.423 for 24-hour analyses, and
0.641 for 48-hour analyses.

The steps for determining if an overlay should be placed during a given season and time are as follows:

- (1) Determine the modulus and thermal coefficient of the existing pavement.
- (2) Select the thickness, modulus, and thermal coefficient of the overlay.
- (3) From laboratory testing or experience, estimate the 7-day interface shear strength.
- (4) Using Figure 6.3, determine the maximum allowable interface shear stress for the desired level of reliability. The maximum allowable tensile stress is one-half the allowable shear stress.
- (5) Compare the maximum allowable stresses from step 4 to the maximum expected stress for the combination of existing slab and overlay material properties shown in Table 6.3.

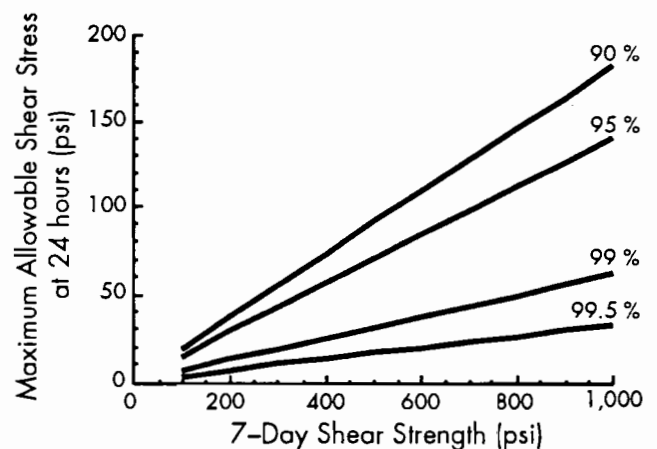


Figure 6.3 Maximum allowable interface shear stress 24 hours after placement for various levels of reliability

- (6) If the allowable stress is greater than the expected stress for all combinations of environment, debonding will not occur, within the limits of the reliability selected.

An example is given below to further clarify the procedure.

If the existing CRC pavement was constructed from siliceous river gravel concrete, then the modulus and the thermal coefficient can be estimated to be 6,000,000 psi and 0.000006 in./in./°F, respectively. If a 4-inch overlay is planned using the same aggregate type, then the modulus and thermal coefficient of the overlay will equal those of the existing slab. Laboratory test results show the direct shear strength to be 600 psi at 7 days for the combination of surface preparation, bonding agent, and overlay concrete to be used. If one-half of one percent delamination can be tolerated, then the maximum allowable shear stress at 24 hours after placement is about 20 psi and the corresponding allowable tensile stress is 10 psi. Comparison of these values with the expected stresses, developed in Ref 2 and summarized in Table 6.3, shows that this overlay should not be placed during winter or summer mornings. However, by changing the overlay aggregate to limestone (4,000,000 psi and 0.000004 in./in./°F), this overlay could be placed throughout the year.

When materials that are used have properties not directly addressed in Table 6.3, stresses can be calculated using the regression analyses shown in Ref 2. This will allow new materials to be considered when overlays are designed. The inferential space is limited to concrete moduli of between 4 and 6 million psi and thermal coefficients between 0.000004 and 0.000006 in./in./°F.

6.3.2 Bonding Agents

The use of bonding agents with overlays is common for many agencies. The laboratory data for overlays placed with latex-modified cement grout, epoxy bonding agent, and portland cement grout and for overlays placed without grout can be found in Ref 2. Given the magnitude of the standard deviations for all combinations, there is no statistical difference in the mean shear strengths. Therefore, based on the laboratory shear strength data, there is no reason to favor one type of bonding agent over another (Note, however, the unsatisfactory performance of the latex-modified grout).

There are differences in the tensile strengths presented in Ref 2. The tensile strengths as characterized by the direct tension test are statistically different; however, when the pull-out test was used, no statistical difference was found between various bonding agents. Thus, there is no reason to favor one bonding agent over the others, based on laboratory test results.

Field experience has demonstrated that overlays can be placed successfully with or without bonding agents. The vast majority of the overlays placed in the Houston area have been placed using portland cement grout. The application of grout results in a slight increase in construction cost, but when properly applied it appears to work well. There is the potential for a problem associated with the application of grout, particularly on hot, dry, or windy days. The grout may dry before the concrete can be placed, effectively creating a layer that prevents, or retards, the development of the interface bond. This problem can be avoided by specifying that the contractor apply grout immediately before placement of the concrete and by maintaining vigilant inspection to assure the requirement is being met. This specification increases the job inspection duties for the owner. The problem could be avoided, and the cost per square yard reduced, if the need for any bonding agent could be eliminated.

The experimental sections placed without grout in Houston are performing well. Laboratory data indicate that no statistical difference exists between shear strengths for grout and no-grout specimens. Therefore, it appears that bonded overlays could be placed without grout, at a lower cost, without an increased risk of delamination.

6.3.3 Curing

Effective curing of concrete is particularly important to the success of bonded overlays. Early and effective application of the curing compound is important for two reasons. First, the curing measures will reduce the early-age moisture losses that result in increased volume changes, thereby decreasing the early-age interfacial stresses. Second, the use of curing measures will reduce the likelihood of the formation of plastic shrinkage cracks. The formation of these cracks is particularly detrimental to the bonded overlay because a one-inch deep shrinkage crack in the overlay may constitute 25 percent of the total thickness. A crack constituting 25 percent of the depth of the concrete is similar to the proportion of the concrete thickness sawn when longitudinal and transverse joints are formed in new construction. The development of some of the non-reflective cracks in the overlay may result from these plastic shrinkage cracks. Because FEM analysis showed that the stresses in the vicinity of a non-reflective crack are similar in magnitude to those near the free edge, measures must be taken to avoid the development of these cracks at early ages.

One method for avoiding these cracks is to limit the rate of water loss from the fresh concrete. The American Concrete Institute (ACI) presents a nomograph to be used to estimate the evaporation rate from fresh concrete using the air and concrete

temperatures, relative humidity, and wind speed. The allowable upper limit recommended by ACI is 0.2 lb/ft²/hour. Unless special measures over and above those for the normal double application of curing compound (120 ft²/gallon) are taken, overlay placement should not be allowed when the evaporation rate is above 0.2 lb/ft²/hour. These special measures would include wet blankets or fog curing.

6.4 SUMMARY

The design, specification, and construction of bonded overlays are evaluated. Based on early-age analysis and field performance, overlays could be constructed at thicknesses of 2, 4, or 6 inches using steel mesh. Field performance of plain and fiber-reinforced experimental sections indicates that these combinations could be used successfully. The modulus and thermal coefficient of the overlay should be less than the modulus and thermal

coefficient of the existing slab. No significant difference in interface strength can be found as the result of the use of shot blasting or cold milling surface preparation techniques, and therefore either could be used successfully. A depth of removal and an average texture depth should be specified.

The seasonal and time-of-placement construction control that relies on the expected 7-day strength for a given combination of surface preparation, bonding agent, and concrete mixture is presented. This technique utilizes the stresses calculated by the FEM program for a specific set of environmental conditions and for an acceptable level of delamination to isolate feasible times and seasons of placement. A bonding agent does not appear to be necessary for the success of bonded overlays at early ages. Curing measures are required to reduce the chance of delamination, and the ACI evaporation rate limit of 0.2 lb/ft²/hour is recommended for use during the construction of bonded overlays.

Table 6.3 Calculated stresses for winter and summer mornings for various combinations of BCO materials

Slab Modulus	Slab Thermal Coef.	Overlay Modulus	Overlay Thermal Coef.	Overlay Stress	Overlay Thickness (in.)	Winter Morning				Summer Morning						
						2		4		2		4				
						Shear	Tensile	Shear	Tensile	Shear	Tensile	Shear	Tensile			
						4	6	4	6	4	6	4	6			
4	4	4	4	4	4	4	11	6	16	12	8	6	9	7		
						6	19	11	25	19	12	9	15	12		
		6	4	4	14	8	18	14	10	7	10	8				
				6	23	12	28	21	14	11	17	13				
		6	6	4	9	6	14	12	8	6	6	6				
				6	17	9	23	19	12	9	13	11				
	6	4	4	4	4	4	4	11	7	17	13	10	7	7	6	
							6	20	11	27	21	14	11	15	12	
		6	6	4	4	4	4	4	11	6	16	13	8	6	9	7
								6	19	11	26	20	12	9	15	12
		6	6	6	4	4	4	4	14	8	19	14	10	7	10	8
								6	23	13	30	22	15	11	18	14
6	6	6	6	4	4	4	9	6	15	12	8	6	6	6		
						6	17	10	24	19	12	9	13	11		
6	6	6	6	6	6	4	11	7	18	13	10	8	8	7		
						6	21	12	29	21	15	11	15	12		

CHAPTER 7. CASE STUDY

7.1 DESIGN OF BCO FOR THE SOUTH LOOP OF IH-610, HOUSTON

Data utilized in designing a BCO for the South Loop of IH-610 in Houston were used to illustrate an example problem (Ref 7). The remaining life was calculated based on a distress index obtained from condition surveys. The estimated number of 18-kip ESAL for a 20-year design life was established at 15,577,000. The existing pavement modulus was back-calculated as approximately 5,000,000 psi, while the overlay modulus was also assumed to be 5,000,000 psi. The average crack spacing was assumed to be 3 feet, while the remaining life was estimated at 80 percent. The existing pavement was 8 inches thick. The modulus of subgrade reaction was assumed to be 250 pci and the flexural tensile strength to be 700 psi.

Table 7.1 shows the stresses calculated for a 2-inch, a 4-inch, and a 6-inch overlay using Equations 4.1, 4.2, and 5.1. The governing stress is selected and used in calculating the number of ESAL the facility can carry before failure. The thickness is then plotted against the number of 18-kip ESAL, as shown in Figure 7.1. From this figure the thickness necessary to last 20 years, or, as evaluated in Figure 7.1, the thickness necessary to last 15,577,000 repetitions of ESAL, can be obtained.

It should be remembered that the equations used for evaluating the stress are based on mechanistic procedures. The equations used to evaluate the long-term performance are based on a selected mechanism of failure, which in this case is 50 feet of cracking per 1,000 square feet of pavement. That is associated with 3 punchouts per mile per year. However, long-term performance data are not available for BCO. Therefore, the performance of BCO should be investigated as the sections surveyed in Houston age, and the long-term performance model used should be upgraded to better reflect the behavior of BCO. Furthermore, the better the method of predicting the remaining life of the pavement, the better the design result. Using a remaining life cal-

culated from a distress index obtained from condition surveys (Ref 7) gives the best results because it relates the actual pavement condition to the remaining life.

From Figure 7.1 it can be concluded that an overlay thickness of approximately 4.5 inches will be adequate to extend the life of the pavement for another 20 years, at which time punchouts will start developing at a rate of approximately 3 per mile per year. The 3 punchouts per mile per year is a structural failure. Increased maintenance can prolong the life of the pavement for another few years. It will, however, be economical to overlay the overlaid pavement after 20 years to get the most out of the pavement.

Table 7.1 Stresses and 18-kip ESAL for example problem

		Overlay Thickness (in.)		
		2	4	6
Stress (psi)	Transverse Stress (Eq 7.2)	154	103	78
	Longitudinal Stress (Eq 6.1)	86	62	47
	Stress in Overlay (Eq 6.2)	-297	-9	29

Traffic (ESAL)	N (Future Predict) (Eq 7.3)	4,355,514	14,439,105	33,385,405
	n (Future) (Eq 7.5)	3,484,411	11,551,284	26,708,324

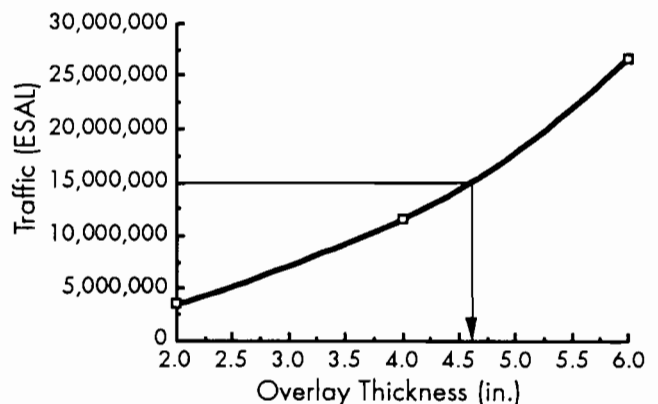


Figure 7.1 Overlay thickness versus 18-kip ESAL

7.2 CONSTRUCTION CONTROLS FOR THE SOUTH LOOP OF IH-610, HOUSTON

The construction controls implemented on the IH-610 South Loop bonded overlay were developed based on observations of the IH-610 North Loop bonded overlay and on discussions with SDHPT personnel familiar with the North Loop project. Details of those observations and the conclusions drawn from them can be found elsewhere (Refs 2 and 3). It is noteworthy that the construction controls used on the IH-610 South Loop overlay project have apparently been successful in preventing early-age delamination. No delamination has been located on this project in the standard overlay, which consists of 4-inch, limestone aggregate, wire-reinforced overlay placed on a cold-milled surface prepped with neat

cement grout. Early-age debonding did occur in an experimental section placed using latex-modified grout. However, this section was removed and replaced with a conventional BCO. Construction controls consisted of the following items.

- (1) The surface was prepared using a cold-milling technique.
- (2) Limestone aggregate was used.
- (3) A limit on the allowable evaporation rate during overlay placement was set at 0.2 lb/ft²/hour.
- (4) The temperature differential between the air temperature at the time of placement and the minimum expected in the 24 hours following placement was limited to 25 degrees.
- (5) A bonding agent consisting of neat cement grout was used throughout the project.

CHAPTER 8. CONCLUSIONS AND RECOMMENDATIONS FOR FUTURE WORK

8.1 CONCLUSIONS

In Chapter 2 it is concluded that delamination of bonded concrete overlays constitutes an early-age problem that occurs the first few weeks after construction. Based on the data from Houston, bonded overlay delamination is not progressive, but the influence on the long-term performance of the pavement is uncertain. Delaminated areas will ultimately need maintenance before areas that are not delaminated, which will have an economic impact.

It can further be concluded that reinforcing type, thickness, and aggregate are important in transverse crack development in bonded concrete overlays and in the development of interface stresses at early ages. Also, different reinforcing procedures produce different crack spacings. Wire-reinforced sections have approximately the same before- and after-overlay crack spacing, while fibers significantly increase crack spacing.

The wheel load stresses were analyzed and an equation developed for stress calculations in BCO. It was further concluded that a BCO will perform in the same way as will a newly constructed pavement, but that the remaining life of the existing pavement influences the stress development of the pavement.

In Chapter 5 a thickness design method for BCO is proposed that is based on fatigue cracking of BCO. The knowledge gained from the statistical analysis of field data, and an analysis using the FEM program, were used to develop the design system. It can also be concluded that BCO should not be placed if the deflections at the crack are more than 1.25 to 1.7 times that between crack deflections.

8.2 RECOMMENDATIONS

It is recommended that the design system proposed in this work be used to design BCO on CRC pavements. The method of establishing whether a BCO should or should not be placed must be used to evaluate existing pavements.

8.3 RECOMMENDATIONS FOR FUTURE WORK

The most important factor not explored, because of the lack of data, is the long-term performance prediction model to be used. Two paths can be followed in future research. Either the existing test sections in Houston can be monitored, and results in 10 to 15 years used to evaluate the long-term performance of BCO, or an accelerated test method can be used. With the advent of the mobile load simulator (MLS) (Ref 3), which is currently under development in Texas, a machine is available that can be used to quickly evaluate the long-term performance of BCO and to verify the model developed in this work.

The effects of time and traffic on the reduction of load transfer at cracks in CRCP are also important, and the MLS can be used in this area as well. This research is needed not only for BCO but also for CRCP.

The influence of temperature on the fatigue life of overlays should be incorporated in a long-term performance model developed for overlays. The temperature stress gives the state of stress the pavement is experiencing as the wheel load passes. The fatigue of concrete depends on the ratio of maximum to minimum stress. An easy method for evaluating this should be developed.

REFERENCES

1. Won, M., "A Mechanistic Model of Continuously Reinforced Concrete Pavement," Research Report 1169-2, Center for Transportation Research, The University of Texas at Austin, 1986.
2. Lundy, J. L., "Delamination of Bonded Concrete Overlays at Early Ages," Research Report 1205-2, Center for Transportation Research, The University of Texas at Austin, 1990.
3. Van Metzinger, W. A., "An Empirical-Mechanistic Design Procedure for the Rehabilitation of Pavements," Research Report 1205-1, Center for Transportation Research, The University of Texas at Austin, 1990.
4. Eisenmann, J., "Westergaard's Theory for Calculation of Traffic Stresses," Workshop on Theoretical Design of Concrete Pavements, Netherlands Center for Research and Contract Standardization in Civil and Traffic Engineering, Epen, The Netherlands, 5-6 June 1986.
5. Voigt, G. F., Carpenter, S. H., and Darter, M. I., "Rehabilitation of Concrete Pavements Vol II: Overlay Rehabilitation Techniques," Report No. FHWA-RD-88-072, Federal Highway Administration.
6. Taute, A., McCullough, B. F., and Hudson, W. R., "Improvements to the Materials Characterization and Fatigue Life Prediction Methods of the Texas Rigid Pavement Overlay Design Procedure," Research Report 249-1, Center for Transportation Research, The University of Texas at Austin, November 1981.
7. "Design Analysis for Rehabilitation of the CRCP on Southeast Quadrant of Houston Loop 610," Unpublished report conducted for the Texas State Department of Highways and Public Transportation, Research Report 920-1, Center for Transportation Research, The University of Texas at Austin, October 1986.
8. Vallabhan, C. V. G., Asik, M., and Rahman, K., "Finite Element Program for Analysis of Bonded Concrete Overlays," Center for Applied Research and Engineering, Texas Tech University, July 1990.

